INITIATION OF MOTION : EFFECT OF ROUGHNESS CONCENTRATION

A Thesis Submitted
in Partial Fulfilment of the Requirements
for the Degree of
MASTER OF TECHNOLOGY

By
MOHD. ASLAM

to the
DEPARTMENT OF CIVIL ENGINEERING
INDIAN INSTITUTE OF TECHNOLOGY, KANPUR
MAY, 1981

CERTIFICATE

The present work entitled 'INITIATION OF MOTION: EFFECT OF ROUGHNESS CONCENTRATION' by Mohd. Aslam is hereby approved as a creditable report on research carried out and presented in a manner which warrants its acceptance as a prerequisite for the degree of MASTER OF TECHNOLOGY. The work has been carried out under my supervision and has not been submitted elsewhere for award of a degree.

May 2, 1981

(Dr. T. Gangadharaiah)
Assistant Professor
Department of Civil Engineering
Indian Institute of Technology, Kanpur

ACKNOWLEDGEMENT

I wish to express my sincerest and deep sense of gratitude to my thesis supervisor Dr. T. Gangadharaiah, for his valuable guidance, constant inspiration and encouragement during the course of the present work.

Sincere thanks are extended to Dr. V. Lakshminarayana, Dr. K. Subramanya and Dr. S. Surya Rao of the Department of Civil Engineering for the thought provoking courses me received from them during the degree programe.

I acknowledge with thanks to Mr. P.D. Porey for his inspiration and keen interest, which made the completion of the present study.

Technical help provided by staff of Hydraulics and Water Resources Laboratory of the Department of Civil Engineering is greatfully acknowledged.

And finally, the unreserved help received from Sri S.P. Sharma is also acknowledged.

Mohd. Aslam

ABSTRACT

The flow conditions corresponding to the initiation of motion of sediment grains in a bed having densely packed with cohesionless sediments have been investigated very systamatically in the past. Threshold flow conditions corresponding to a particular grain size, resting on a particular level with respect to general surface of the bed in a less dense bed have not been investigated. An attempt has been made to investigate for these flow conditions in the present work.

The experimental programme of the present work covers three aspects; namely, the effect of roughness concentration, effect of size variation of a particular grain incomparision to grains constituting bed roughness and the effect of relative position of the grain of same size that of roughness elements on their initiation of motion. The following are the significant outcomes of this investigation.

The drag co-efficient calculated from the mean velocity data found to increase with decrease in roughness concentration, λ , and tends to be independent of roughness concertration for $\lambda < 0.1$. The theoretical bed level found to coincide with the average surface level of the rough bed.

The decrease in roughness concentration, the increase in grain size, and the increase in elevation of grain, result in the reduction in critical shear stress, τ_* based on the average bed shear stress. However, critical shear stress e xpressed interms of shear stress, τ_{*r}, offered by a particular grain under investigation agrees with Shields critical shear stress value.

CONTENTS

FIGURES

NOTATIONS

B, B_s, B_r	Constants
C_1	Constant
d	Diameter of glass bead
D	Center to center spacing of glass bead.
d_i	Variable diameter of glass bead.
g	Acceleration due to gravity
$\bar{h}$	Average height of roughness element
K_s	Nikuradse's equivalent sand grain roughness
R_*	$\frac{V_* d}{\nu}$ Shear Reynolds number.
r,R.	Suffixes for rough bed
s,S.	Suffixes for smooth bed
u	Average velocity at any height
V_*	Shear velocity $V_* = \sqrt{\tau_0/\rho}$
$\frac{\Delta u}{V_*}$	Intercept of law of wall
Y	Ordinate, distance measured perpendicular to the bed from the top of grain.
$Y_t = (Y + \varepsilon)$	Perpendicular height from theoritical bed level.

Greek alphabets

δ	Boundary layer thickness measured from the top of the grain.
ε	The location of the apparent origin from velocity distribution above the smooth surface of the flat bed.
κ	Von Karman's universal constant
ρ	Mass density of the fluid
ρ_s	Mass density of glass bead
τ_o	Bed shear stress
τ_{*c}	Non-dimensionalised critical shear stress.
τ_{*r}	Non-dimensionalised critical shear stress offered by single particle
ν	Kinematic viscosity
λ	Roughness concentration

CHAPTER - 1

INTRODUCTION AND LITERATURE REVIEW

1.1 Introduction:

Initiation of motion of sediment is a starting step of sediment transportation. An extensive work has been carried out by various investigators to find the general conditions at which the whole sediment bed is subjected to motion. In cohesionless bed, the sediment motion occurs by the movement of individual sediment grains. The knowledge of flow characteristics on the initiation of motion of grains in a densely packed sediment bed are available due to a systematic investigations carried out in the past. It is not known how the flow conditions at the initiation of motion of sediment particle in a less dense bed differs from that densly packed bed. Further, very little information is available on how the relative size and position of grain alters the critical condition. A knowledge on these characteristics are in need for proper understanding of the mechanics sediment transportation.

The fluid flowing over a bed of cohesionless sediment, exerts a fluid dynamic force on the grains and tends to move or entrain them. The force resisting the motion of cohesionless sediment is mainly due to their weight. When the fluid dynamic forces (Drag force and Lift force) acting on a sediment grain attains a particular value and if that value is increased slightly, the grain will be subjected to the motion. This state of motion of sediment is called 'Initiation of motion' or 'Critical conditin' or 'threshold condition'. This threshold condition is a result of combined action of drag & lift forces on the submerged weight of the grain in cohesionless sediment bed. The drag and lift forces acting on the grain depends upon the roughness charactiristics of the bed and size of grain and its relative position with respect to the average bed surface. The relative spacing of the grains on the bed may be represented as roughness concentration, which is defined as the ratio, of the projected area of roughness elements perpendicular to the flow to the floor area.

Investigations on initiation of motion are generally carriedout for the conditions of the general motion of grains in the densely packed sediment bed. A few attempts have been made to investigate the threshold condition of a single grain resting either on densely packed sediment grain bed or on the smooth bed. Almost no investgation has been carried out to find the influence of roughness concentration and size variation on the threshold condition of an individual grains. In the present investigation an attempt has been made to study the influence of roughness concentration, size variation and its relative position on the threshold condition of the grain under observation.

1.2 Literature Review.

Initiation of motion is one of the major aspects of sediment transport. This problem of initiation of motion has been analysed by several investigators and attempts have been made to develop relation between critical tractive force, sediment size and sediment characteristics such as specific weight. The best known and widely accepted theory on the initiation of motion was proposed by Shields (1936). Vanoni (1977) summarizes the recent contributions of various investigators on this aspect of the problem. A brief review of literature on the effects of roughness concentration, size variations and relative positions of sediment on initiation of motion has been carried out in the following paragraphs.

a. Effect of concentration:

The initiationof motion for the bed of maximum roughness concentration (densest bed) has been analysed by several investigators such as Shields (1936), White (1940) Kurihara (1948), Iwagki (1956) and Egiazaraff (1965) Initiation of motion of a single sediment grain resting on smooth bed has been analysed by Andreas Muller, Albert Gyr, & Themistocles Dracos (1971) They studied the forces on single grain in a turbulent flow. It may be observed that the effect of roughness concentration between the above extreme conditions has hot been investigated. Here an attempt has been made to determine the effect of roughness concentration on the state of initiation of sediment motion.

b. Effect of size variation:

The problem of initiation of motion on densest bed of roughness elements of nonuniform size was studied by Kramer (Ref 8), USWES (Ref 8), Chang (Ref 8) Indri(Ref.8) ,Aki(Ref.8) (Ref.8) Sakai(Ref.8) , Sato and Kurihara (Garde and Raju 1977). The study of Kramer, USWES and Chang indicates that the nonuiformity in size causes an increase in critical shear stress. However, the data of Aki and Sato shows that critical shearstress for non-uniform sediment is less than the uniform sediment. In these investigations the threshold condition is always refered to the medium size of sediment. The initiation of motion of a perticular size of sediment in a nonuniform bed was studied by Egiazaraff (1967).

It may be noted that the effect of size variation of a single grain, subjected to initiation of motion in a given bed of uniform size of roughness element, has not been investigated. Here an attempt has been made to study this problem.

c. Effect of relative position:

The effect of relative position (degree of exposure) of individual roughness element on initiation of motion of cohesionless grain was cansidered by Fenton and Abbott. (1977). They conducted the experiments to measure the dimentionless critical shear stress and its dependence on grain protrusion which was found to be very marked. The critical shear stress of a grain resting on the top of an otherwise flat bed in turbulent stream was measured and found to be 0.01 which is considerably less than previously reported values of 0.03-0.06 for a bed where all the grains were at the same level.

It may be noted from the above that initiation of motion of a roughness element depends upon the bed characteristics like relative concentration, relative position of roughness elements. These characteristics modify the velocity distribution near the bed. Hence it is of importance to study the effect of bed characteristics in the velocity distribution near the bed.

d. Velocity distribution near the bed :

The initiation of motion is controlled by the flow conditions and the later are controlled by the roughness characteristics of the bed surface and the state of flow. So a brief review of the roughness charectaristics of the bed are being carried out here.

Nikuradse (1933) found that the velocity distribution on a bed having uniform sand grains densly packed can be represented in termes of sand grain size K

$$\frac{u}{V_*} = \frac{1}{\kappa} \ln \frac{Y}{K} + B \left(\frac{KV_*}{\nu} \right) \quad .. (1)$$

Where u is mean velocity, V_*- Shear velocity and B is roughness constant, function of $\left(\frac{KV_*}{\nu} \right)$, and velocity destribution near the wall is logarithemic which is universal in character and is determind only from wall conditions.

To characterise the roughness from other type of roughnesses with different roughness concentration, Schlichting used equivalent sand grain roughness K_s and wall Law equation (1) can be written as below:

$$\frac{u}{V_*} = \frac{1}{\kappa} \ln \frac{Y}{K_s} + B \left(\frac{K_s V_*}{\nu} \right) \quad .. (2)$$

Schlichting, Oloughin and Macdonald (1964), David (1980) and Sarin (1980) observed that maximum roughness occurs not at maximum roughness concentration on the bed but at a considerably small value.

e. Vartical Shift in the Law of wall :

Hama (1954) expresed the effect of rough wall region as a vertical shift from smooth wall log law, and can be expressed as below :

$$\left(\frac{u}{V_*}\right)_S - \left(\frac{u}{V_*}\right)_R = \frac{\Delta u}{V_*} = 1/\kappa \ln\left(\frac{K_s V_*}{\nu}\right) + (B_s - B_r)$$

or $$\frac{\Delta u}{V_*} = \frac{1}{\kappa} \ln \frac{V_* d}{\nu} + (B_s' - B_r')$$

Batterman (1965), David, Sarin showed that $\left(\frac{\Delta u}{V_*} - \frac{1}{\kappa} \ln \frac{V_* d}{\nu}\right)$ is a function of roughness concentration λ, variation of $\left(\frac{\Delta u}{V_*} - \frac{1}{\kappa} \ln \frac{V_* d}{\nu}\right)$ with λ shows a definite relationship.

f. Apparent shift in the origin for rough boundrey (ε) below the top of roughness element or Theoritical bed level.

The rough wall law behaves as if its origin is located some distance ε below the crest of element (More 1951) The shift in origin by distance (ε) gives a logarithmic distribution near the wall. Perry, Schefield and Joubert (1969) suggested a trial and error method for finding ε They obtained a relation for closely placed two dimentional strip roughness $\frac{\Delta u}{V_*} = \frac{1}{\kappa} \ln \frac{V_* \varepsilon}{\nu} + C_1$

The constent C_1 in the equation depends upon the geometry of roughness element and has an average value of 0.40. David and Sarin showed that the constant is a function of roughness concentration.

g. Present Investigation:

The experimental programme is planned to study the effect of relative concentration, size and position on the

initiation of a single particle on a bed of uniform size glass beads as roughness elements. This study will be based on flow parameters deduced from the mean velocity profiles measured for the critical condition of a particle.

CHAPTER - 2

EXPERIMENTAL PROGRAMME AND DATA REDUCTION

The details of the present investigation, such as description of experimental setup, details of glass bead beds, measurement of mean velocity and detection critical condition for the glass bead motion are given under the experimental programme.

Deductions of wall law parameters and computation of parameters for the initiation of motion have been presented under data reduction.

2.1 Experimental Programme:

a. Details of Experimental Setup:

In the present investigation the rectangular flume of 15 cm width and 3.0 m length has been used. The system of flow straightners are located at upstream end of the flume. The water is pumped by a motor through venturimentered pipe which enters into the test section via flow straightners for maintaining more or less constant depth of flow vertical steel rods of 10 mm diameter and 25 mm, centre to centre are provided at down stream end of flume.

To control the velocity and depth of flow keeping discharge constant a drilled Alluminium plate of 15x30 cm section used at the discharging end. The discharge is controlled by sluice valve fitted in the supply pipe. The flume body is resting on the lever at centre and is simply supported at the upstream end. The downstream end is cantilevered, which has been made simply supported to remove the defect

of bending by self load of flume and the live load of water. point gauge has been used for measuring the depth of flow which can move along the flume length. The test section has been chosen at 2m. d/s from the inlet. A schematic layout is shown in Fig. 1. and plate-2.

b. Details of glass beads beds:

A 3.0m long and 15cm wide Aluminium plate has been used for sticking the glass beads of 6.5 mm diameter as a roughness element to provide the rough bed. A gride of 1cmx1cm. has been drawn for sticking glass beads in a regular pattern and getting bed of different roughness concentration. Five beds of different concentrations have been made by sticking glass beads in different spacings and arrangments as given in table 1. For the first bed 4 cm centre to centre staggered pattern, for the second bed 2cm center to center staggred pattern, for the third bed 1cm center to center symmetrical pattern, for the fourth bed 1cm. center to center staggered pattern and for the fifth bed densely packed arrangement of glass beads have been used. After sticking the glass beads on plate, this bed is placed on the bed of flume and is tightened by nut and bolt. Prepared glass bead beds are shown in Plate-3

c. Measurment of mean velocity:

A Pitot tube with gauge arrangement was used for measuring the velocity profile. A 30^0 inclined manometer

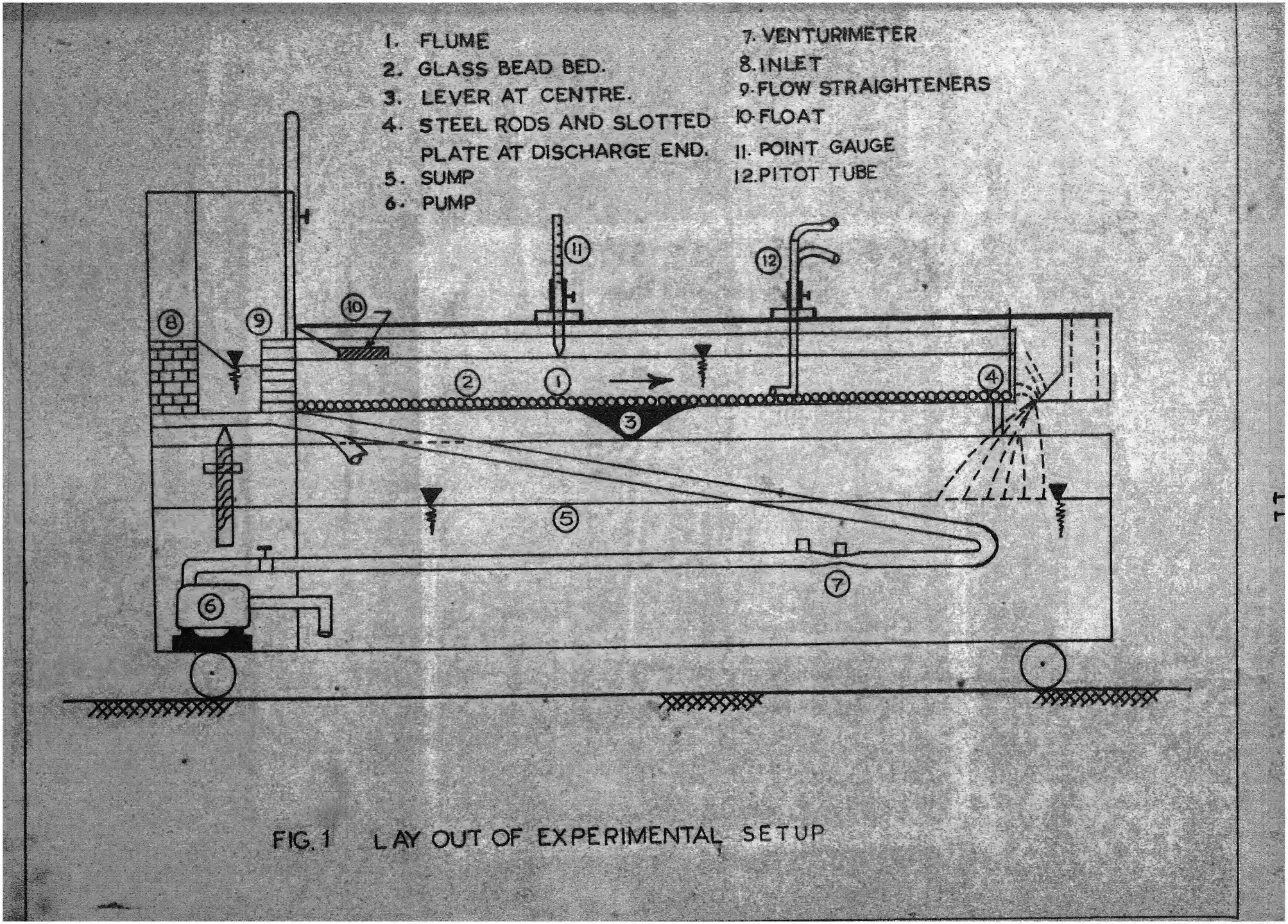

FIG. 1 LAY OUT OF EXPERIMENTAL SETUP

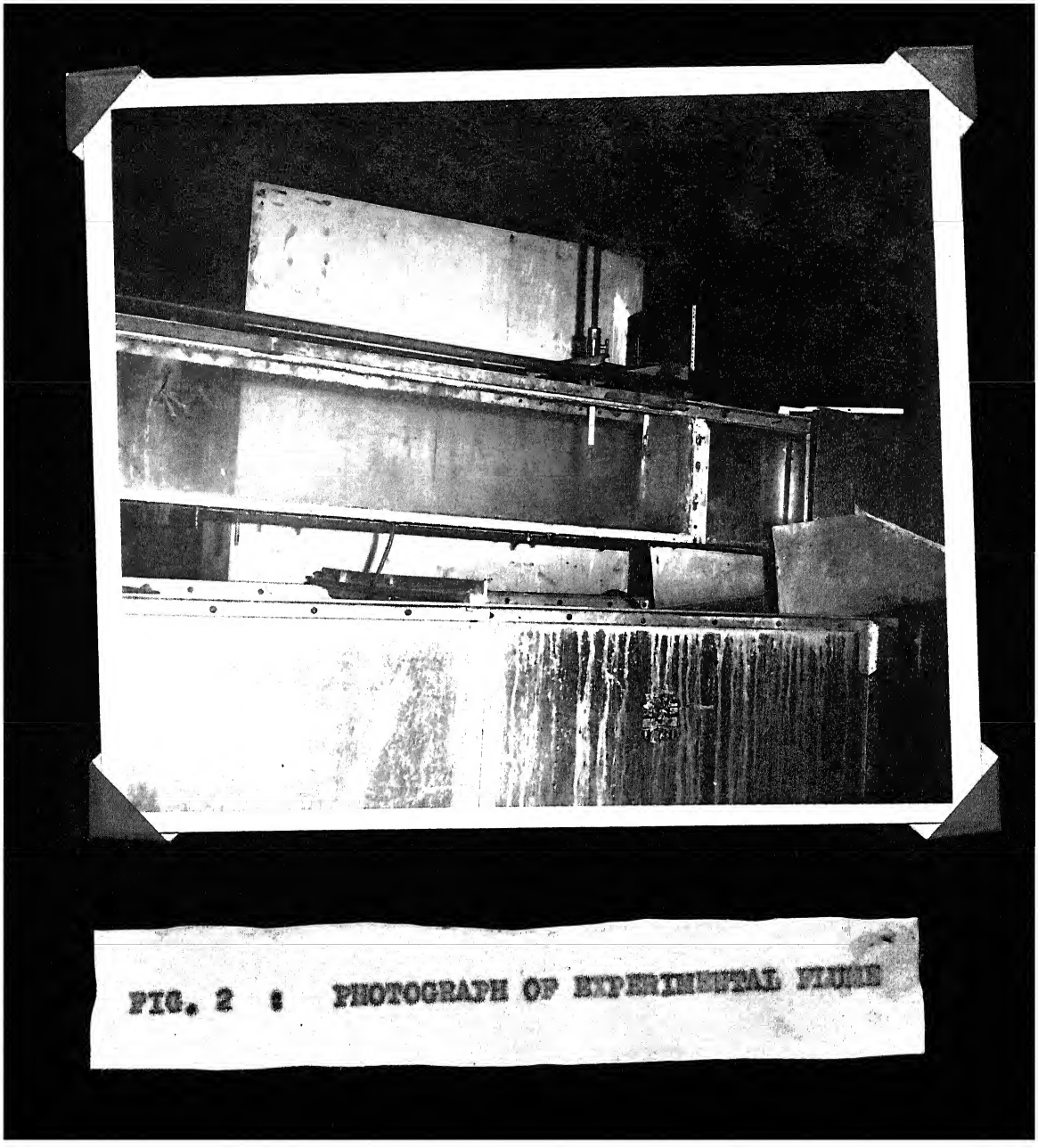

FIG. 2 : PHOTOGRAPH OF EXPERIMENTAL FLUME

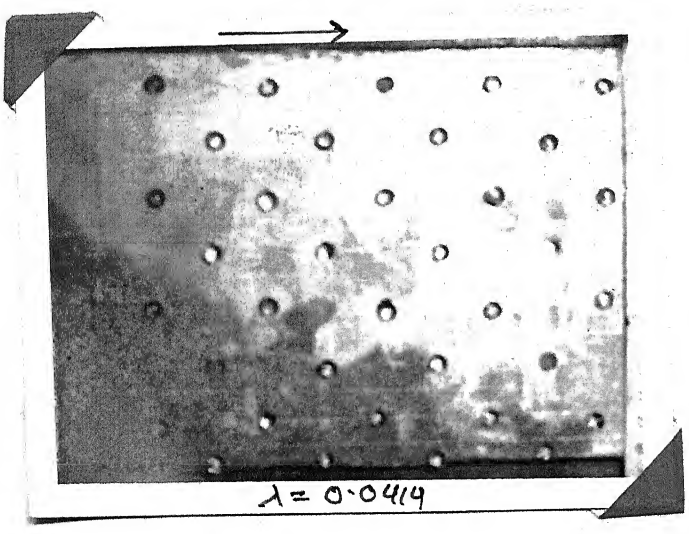

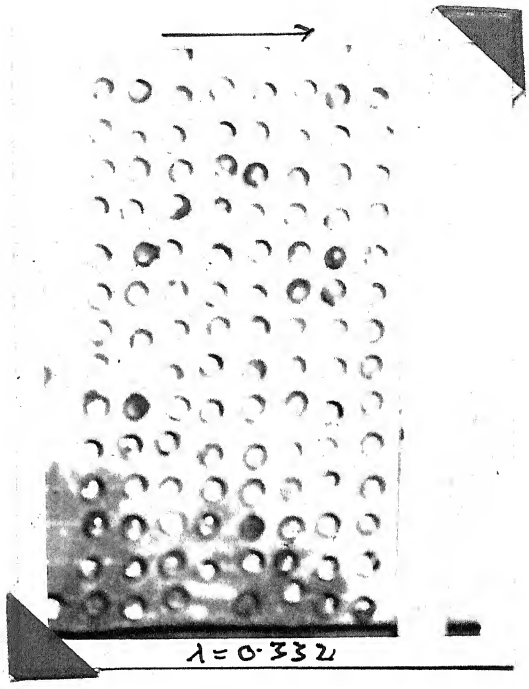

p.13 FIG. 3 : PHOTOGRAPHS OF DIFFERENT DENSITY GLASS BEAD BEADS

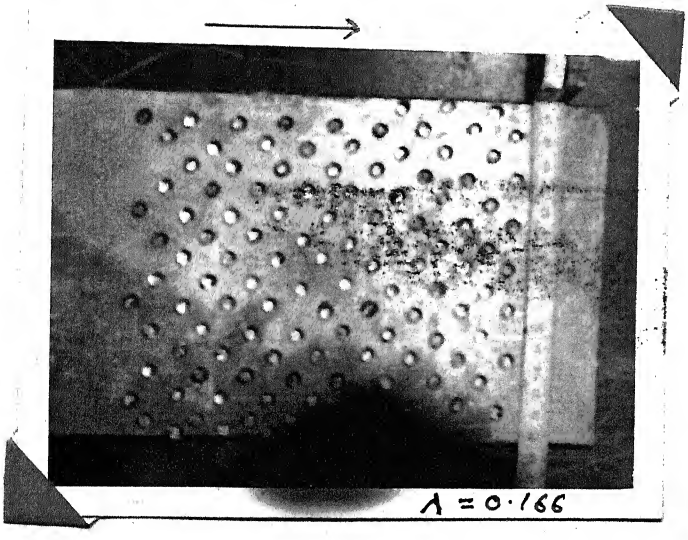

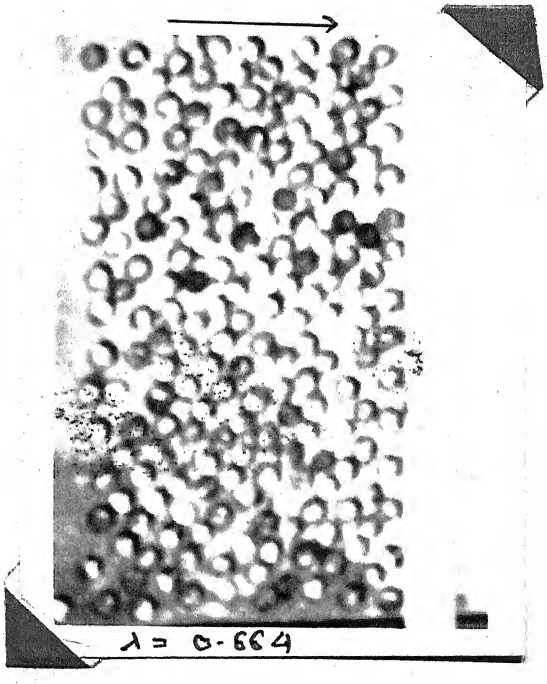

was used, for measuring the velocity heads. For location of zero position of the probe it is gradually lowered down to the position where the pitot tube (probe) is just in touch with glass bead top. This is taken as the zero position of the probe. The probe has been moved upwerd gradually from this position with closer interval for measuring velocity distrition.

d. Discharge measurment:

A calibrated venturimeter which is fitted in supply pipe, was used for measuring discharge.

e. Slope measurment:

The simple support at u/S end of flume also works as slope controlling device as shown in the Fig 1
For measuring the slope, the d/s end of flume is shuttered by a plate and some water is pumped in to the section. While no flow is there, depth of water was measured at each 25cm. interval along the length of the channel. From these measuments slope of bed was calculated.

Details of glass bead beds

Sl. No.	diameter of glass beads	C/C distance.	Type of Arrangement.	Density	Density calculation for Staggered and Symmetrical patterns.
1.	6.5mm.	4cm.	Staggered	0.41	
2.	6.5mm.	2cm.	Staggered	0.166	
3.	6.5mm.	1cm.	Symmetrical	0.332	
4.	6.5mm.	1cm.	Staggered	0.63	
5.	6.5mm. 4.8mm. 4.5mm.	densily packed	densily packed	0.753	

Area of shaded portion
$= D/2^{\frac{1}{2}} \times D/2^{\frac{1}{2}} = D^2/2$

Area of bead
$= (\pi/4)d^2$

$= \frac{(\pi/4)d^2}{D^2/2}$

Area of shaded portion D_1^2

Area of bead $= (\pi/4)d^2$

$= \frac{(\pi/4)d^2}{D_1^2}$

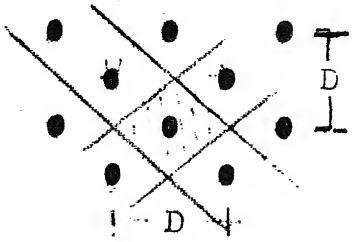

Staggered Pattern

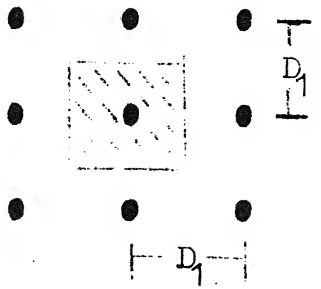

Symmetrical Pattern

f. Detection of critical condition for the glass bead motion:

Usually initiation of motion is detected by the plot of τ_* against sediment discharge (Paintal, 1971). However in the present investigation, the approach based on the motion of individual roughness element has been used. In this approach the critical condition is said to have reached when the fluid dynamic force acting on the grain increased slightly, the grain will be subjected to the motion. The mean velocity profiles justat the up stream of roughness element are measured for this flow condition. The bed shear stress, τ_* roughness characteristics, Ks, and ϵ are computed from these velocity profiles.

2.2 DATA REDUCTION :

Velocity measurement were carried out on 4 different densities of glass bead beds, at center line of flume for different situations of initiation of glass bead motion. These velocity measurements are used in deduction of theoretical bed level (ϵ) , shear velocity (V_*), and roughness function like $\frac{\Delta u}{V_*}$ & $\frac{Ks}{d}$.

Using the computed values of V_* Sheildscritical shear stress parameter $\tau_{*c} = \frac{\rho V_*^2}{(\rho_s - \rho)\, gd}$ and grain shear Reynolds number $R_* = \frac{u_* d}{\nu}$ was calculated.

a. Deduction of wall Law parameters:

Boundry layerflow can be broadly devided in to two regions, namely wall law region and defect law region.

The wall law region extended from wall to a distance of $\frac{Y}{\delta} \simeq 0.2$ and the remaining portion of a boundry layer is represented as defect law region. A portion of the wall law region is represented by a lagarithmic velocity distribution which ranges from $Y/\delta = 0.05$ to 0.20. Lagarithmic velocity distribution is universal in charactar and it is the function of wall characteristics like bed shear velocity V_*, roughness function $\frac{\Delta \bar{u}}{V_*}$ and theoritical bed level ϵ, These characteristics are determined from logarithmic velocity distribution near the wall.

b. Theoritical Bed level (ϵ)

In the case of rough wall flow, it has been found by Moore (1951), Perry, Joubert (1963) and Liu etal (1966) that the logarithmic profile still exists provided that the Y origion is located at a distance ϵ below the crest of the roughness element i.e. $Y_t = Y + \epsilon$, where Y is measured from the top of roughness element. In the present analysis, a graphical method is used for the determination of ϵ and shear velocity V_*. The basic steps required to determine ϵ and V_* using the graphical method are:

1. The orgin for $Y_t = Y + \epsilon$ is chosen by trial and error to give the closest approximation to linearity in the semi logarithmic graph.

2. The best straight line is drawn through the resulting plot;

c. Shear Velocity V_*

Shear velocity is defined as $V_* = \sqrt{\frac{\tau_o}{\rho}}$ in which τ_o is bed shear stress and ρ is fluid density. The slope of the best fitted straight line in the plot of u against In Y_t gives the value of $\frac{V_*}{\kappa}$. The value of V_* is computed for the Karman constant $\kappa = 0.40$ from, above computed slope. The bed shear stress τ_o is computed using the relation.

$V_* = \sqrt{\frac{\tau_o}{\rho}}$ in which ρ is density of fluid.

d. Roughness function $\Delta u/V_*$

The roughness effect $\Delta u/V_*$, represents the down word displacement of the logarithmic portion of the plot of rough-wall law $\frac{u}{V_*}$ with $\frac{(Y+\varepsilon)V_*}{\nu}$ from the smooth wall log law.

The smooth wall log law is represented by equation as below.

$$\frac{\bar{u}}{V_*} = \frac{1}{\kappa} \text{ In } \frac{YV_*}{\nu} + 5.5 \qquad \text{------ (1)}$$

And wall low for rough bed may be represented by relation.

$$\frac{\bar{u}}{V_*} = \frac{1}{\kappa} \text{ In } \frac{(Y+\varepsilon)V_*}{\nu} + 5.5 - \frac{\Delta u}{V_*} \qquad \text{--- (2)}$$

The vertical shift of rough wall low eqn (2) from smooth wall law eqn (1) is measured from the plot $\frac{\bar{u}}{V_*}$ with $\frac{(Y+\varepsilon)V_*}{\nu}$ in Fig 4A . 4B

e. Equivalent sand grain Roughness (K_s)

For hydrodynamically smooth and rough boundaries, well known velocity distribution equation given by Prandtl and Karaman as wall law:

For Smooth boundries :- $\left(\frac{u}{V_*}\right)_S = 5.75 \log \frac{V_* Y}{\nu} + 5.5.$ ...(1)

For rough boundries: $\left(\frac{u}{V_*}\right)_R = 5.75 \log \frac{Y}{k_s} + 8.5$ ...(3)

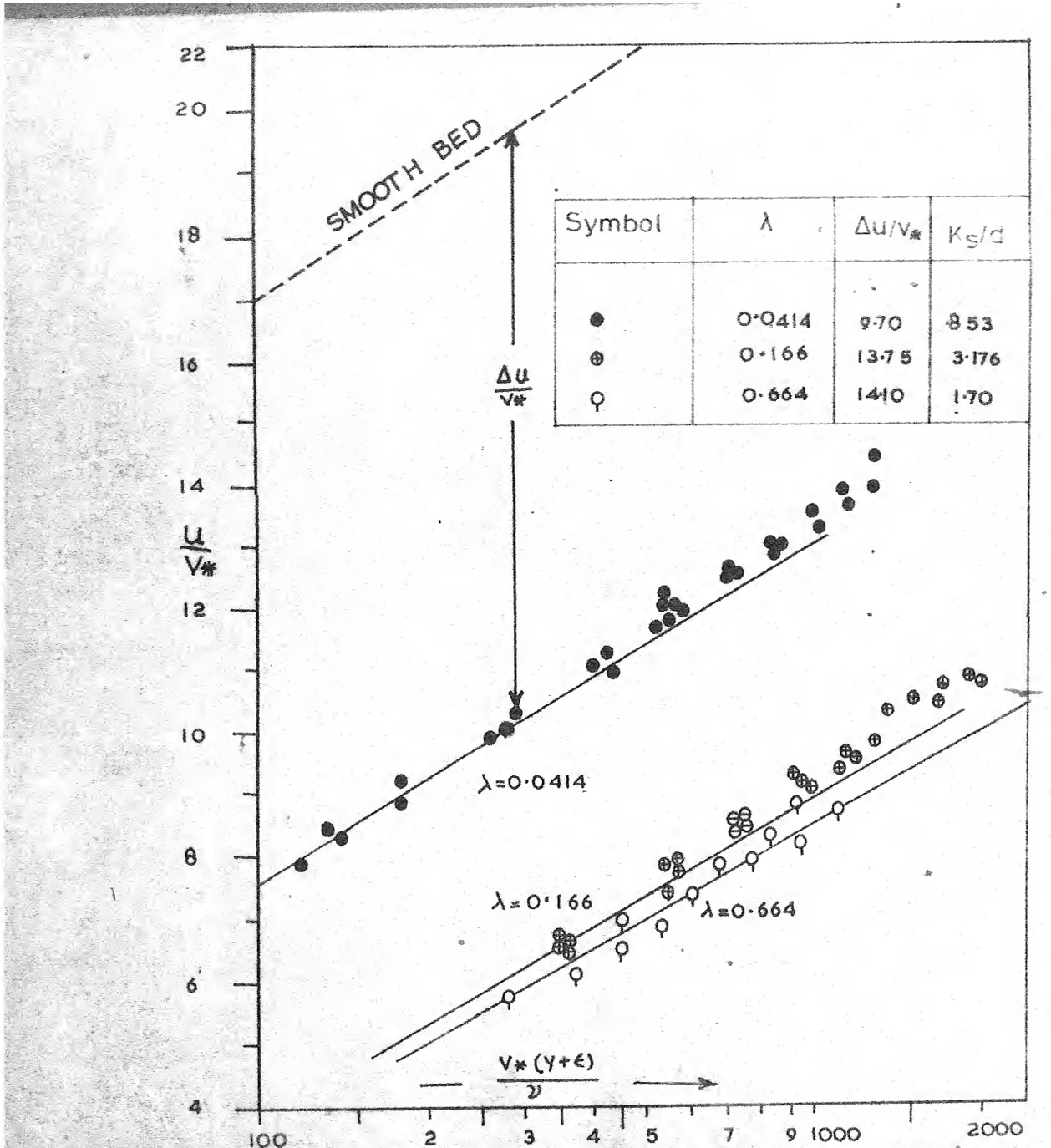

FIG. 4-A SHIFT IN VELOCITY DISTRIBUTION FROM A SMOOTH WALL LAW (A-1)

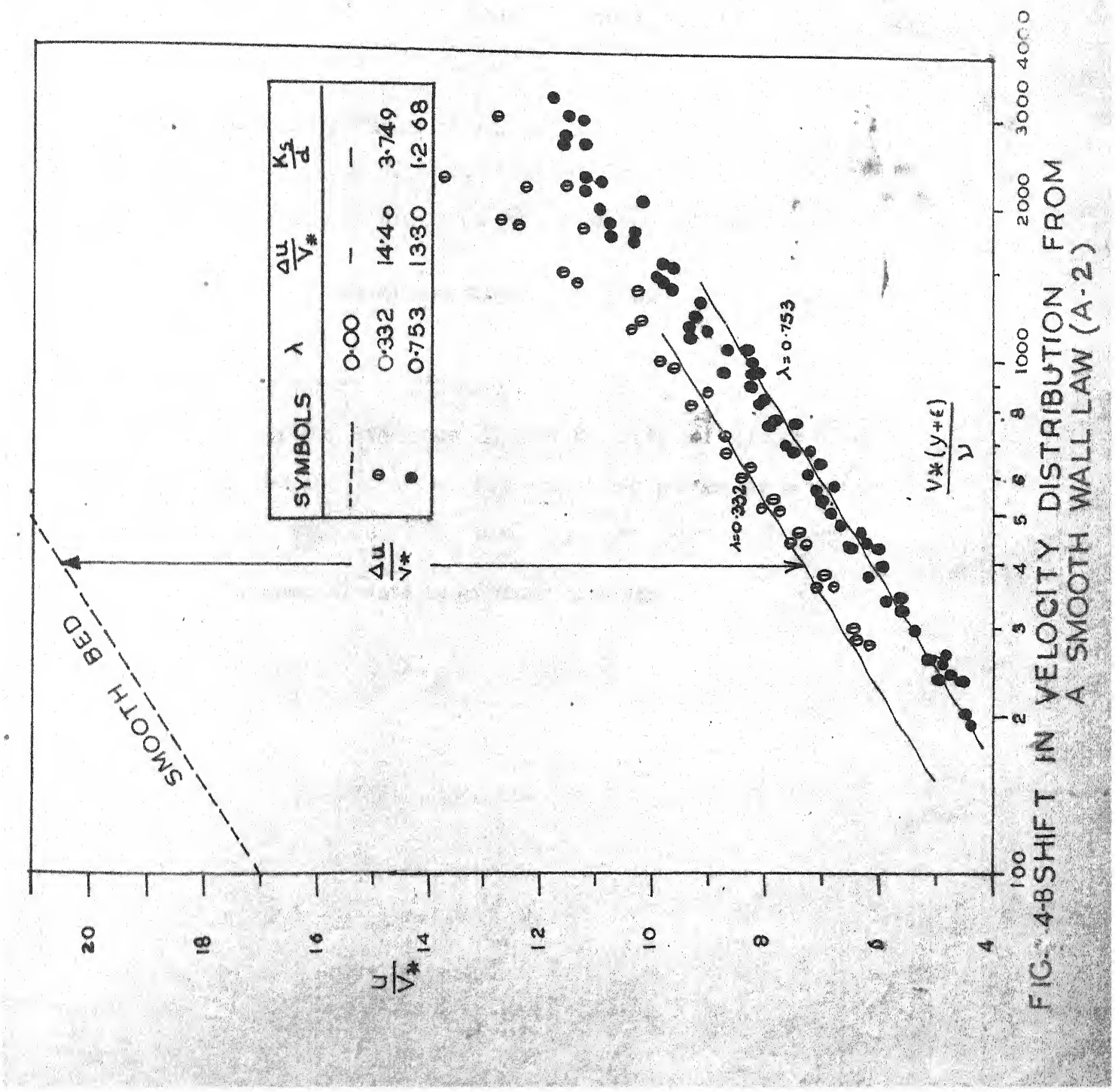

FIG.-4-8 SHIFT IN VELOCITY DISTRIBUTION FROM A SMOOTH WALL LAW (A-2)

From these two equations (1) & (3) we can get

$$\frac{\Delta u}{V_*} = \left(\frac{u}{V_*}\right)_S - \left(\frac{u}{V_*}\right)_R = 5.75 \log \frac{V_* k_s}{\nu} - 3.0$$

Ks can be calculated from this equation using the computed values of Δu and V_*.

f. Parameters for the initiation of motion

Initiation of motion of sediment was represented by Shields (1936) in terms of shear stress parameters

$$\tau_* = \frac{V_*^2}{\left(\frac{\rho_s}{\rho} - 1\right) gd}$$ and grain shear Reynolds number

$R_* = \frac{V_* d}{\nu}$. using the computed value of V_*, and measured values of grain diameter d, and density of glass bead and known value of ρ for water at given temperature, the values of R_* and τ_* have been computed.

Experimental data is given in Appendix.

CHAPTER-3

ANALYSIS OF EXPERIMENTAL RESULTS

The experimental results have been analysed in the following sequence:

1. Effect of roughness concentration on the mean velocity distribution and their roughness scales.
2. Effect of Roughness concentration on the initiation of motion of glass bead.
3. Effect of size variation of single particle(glass bead) in given bed on its initiation of motion.
4. Effect of relative position of single particle on its initiation of motion.

1.1 Mean velocity Distribution:

The mean velocity profiles measured near the bed for the different roughness concentrations are presented in two methods as indicated in the introduction. In the first method, the velocity profile is represented interms of shift in velocity namely $\frac{\Delta u}{V_*}$, as

$$\frac{\Delta u}{V_*} = \frac{1}{\kappa} \ln \left(\frac{y+\varepsilon}{\nu} V_* \right) + 5.5 - \frac{u}{V_*} \qquad ..(1)$$

Incorporating the velocity shift $\frac{\Delta u}{V_*}$ with velocity profiles as

$$\frac{u+\Delta u}{V_*} = \frac{1}{\kappa} \ln \left(\frac{y+\varepsilon}{\nu} \right) V_* + 5.5 \qquad ...(1a)$$

and plotting $\frac{u+\Delta u}{V_*}$ against $\left(\frac{y+\varepsilon}{\nu}\right) V_*$ in fig. 5 for all beds of various roughness concentrations, it may be observed that the experimental data agrees fairly with Eqn. 1a.

In the second method of presentation, the velocity profile is represented interms Nikuradse's equivalent sand grain roughness k_s, as

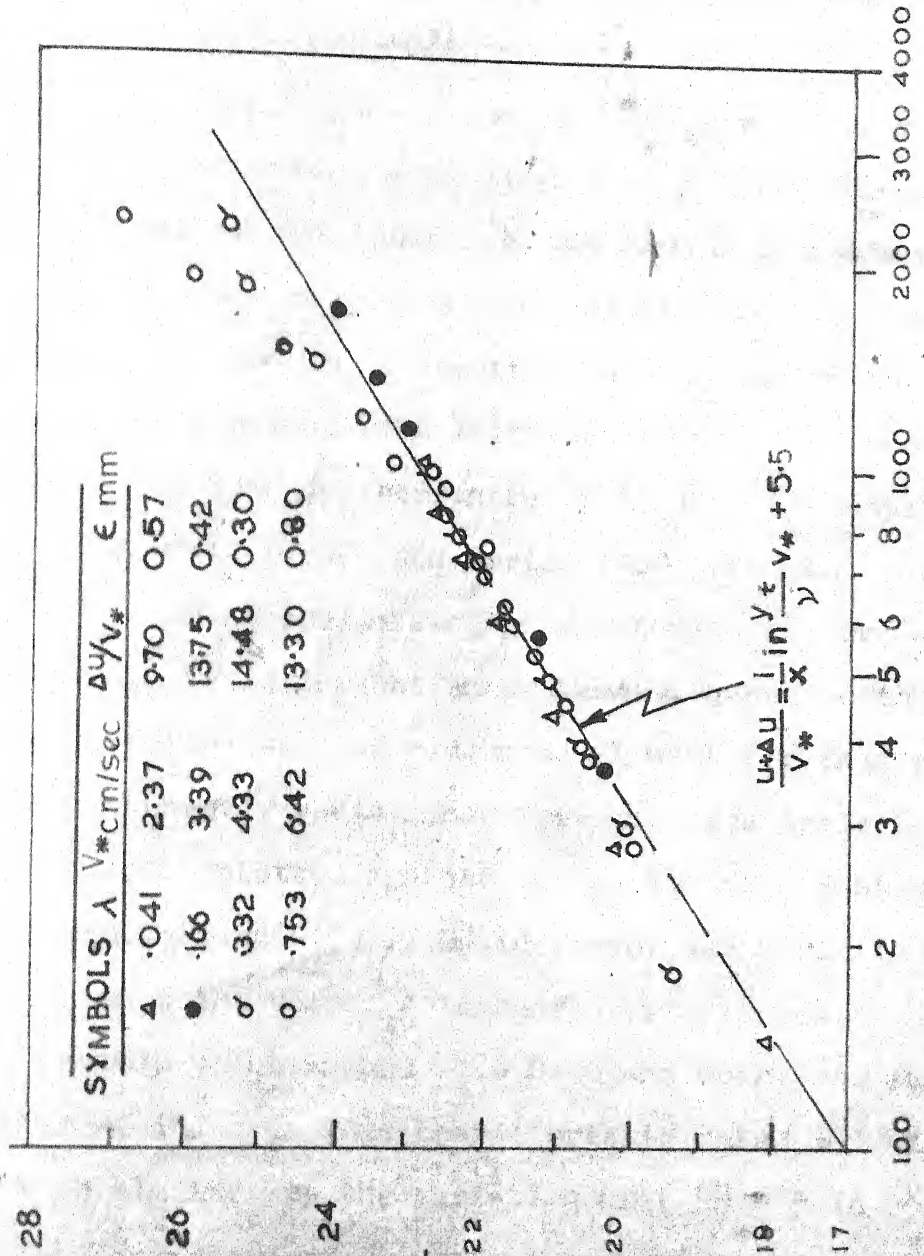

FIG.5 LAW OF WALL

$$\frac{u}{V_*} = \frac{I}{\kappa} \ln \left(\frac{y+\varepsilon}{k_s}\right) + B \qquad \ldots\ (2)$$

The experimental data plotted in the form of $\frac{u}{V_*}$ against $\frac{Y_+}{k_s} = \frac{y+\varepsilon}{k_s}$ in Fig. 6 agrees fairly with the eqn (2)

1.2 Effect of Roughness concentration on Roughness scales:

a. The roughness scales used in representing the velocity profiles as shown in figs 5,6 are $\frac{\Delta u}{V_*}$ and $\frac{K_s}{d}$. These scales are found to be the function of roughness concentration. The roughness scale plotted in the form $(\frac{\Delta u}{V_*} - \frac{I}{\kappa} \ln \frac{dv_*}{\nu})$ against roughness concentration λ as shown in Fig. 7 is found to increase with increase of λ upto $\lambda = 0.26$, and then decreases with further increase in λ. The data of Schlichting (1937) David (1980) and Sarin (1980) are also incorpated in Fig. 7, which shows fair agreement with the present investigation. David present an explanation based on the variation of effective area of roughness element for this particular characteristic variation. The roughness scale presented interms of k_s/d is plotted against λ in the Fig. 8 alongwith the data of Schlichting (1937), David (1980) and Sarin (1980). It is seen that the value $\frac{K_s}{d}$ increases with increase in λ, attains a maximim value around $\lambda = 0.26$ and decreases further with increse in λ. This characteristic relation of k_s/d with λ is similar to the variation of $(\frac{\Delta u}{V_*} - \frac{I}{\kappa} \ln \frac{dv_*}{\nu})$ with λ

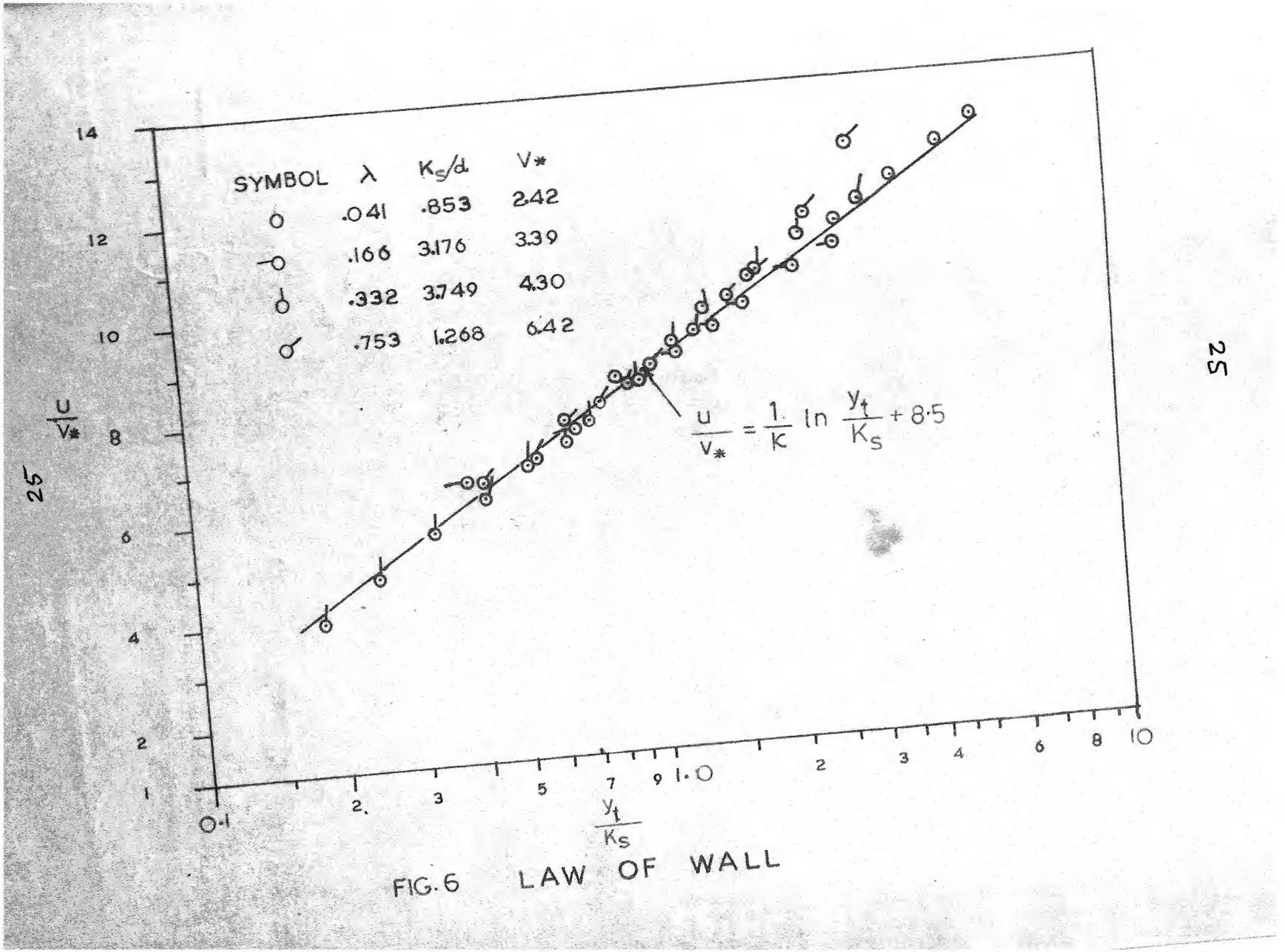

FIG. 6 LAW OF WALL

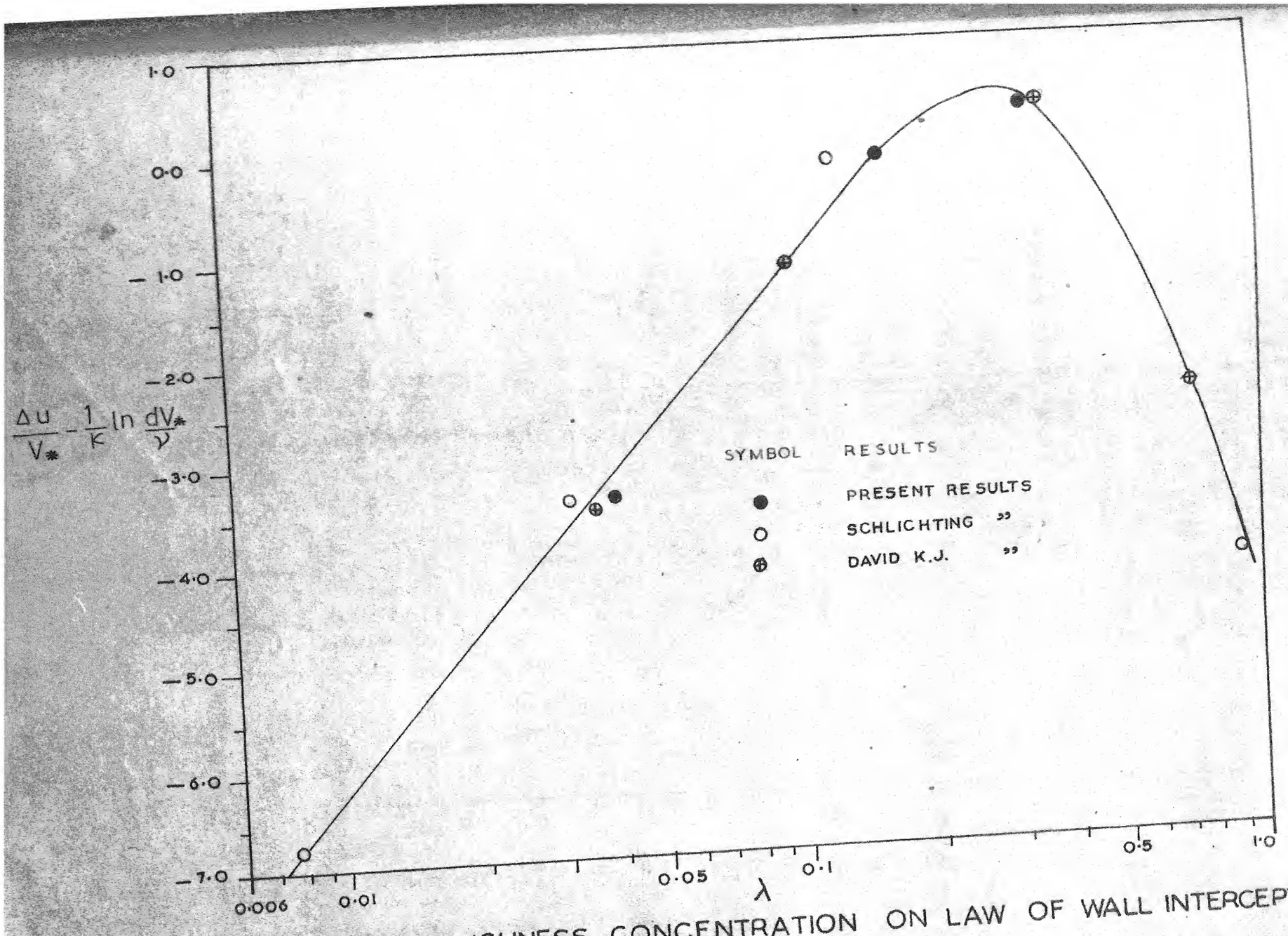

FIG. 7 EFFECT OF ROUGHNESS CONCENTRATION ON LAW OF WALL INTERCEPT

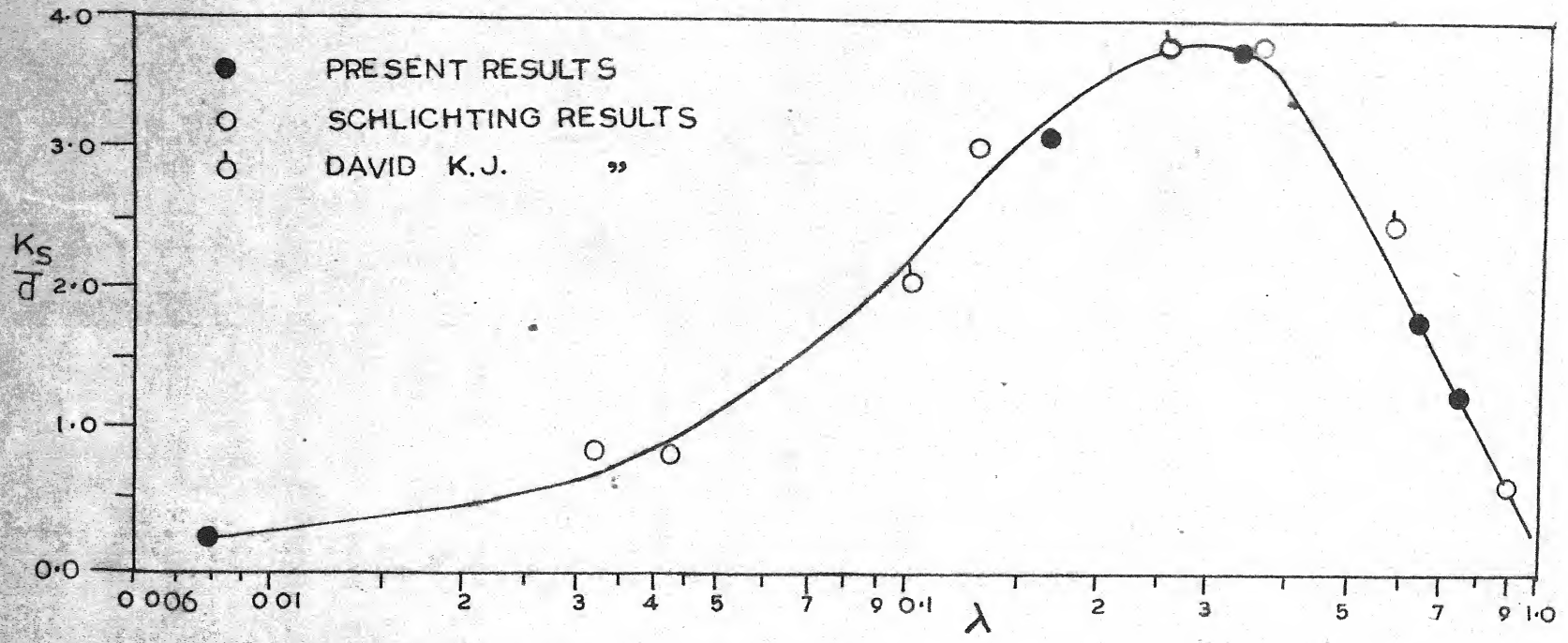

FIG. 8 EFFECT OF ROUGHNESS CONCENTRATION ON K_s

b. Theoritical Bed level ε

The apparent origin or the theoritical bed level of the logarithmic velocity distribution situated below the top of the roughness element is of impartance in the computation of fluid dynamic force acting on roughness element. The location of this origin depends upon the size and roughness concentration of sedement bed. Bayinco and Partheniades (1971) gave a relation $\varepsilon = 0.25\ K_s$ for the location of apparent origin below the top of bed surface in which sediment grains are densely packed. The Theoretical bed level is found to vary with roughness concentration on the bed, as shown in Fig. 9 It may be observed that as the roughness concentration decreases the thearetical bed level moves towards bottom of roughness element. Data of David and Sarin have also been incorporated in this figure. In the same figure, the surface level of the rough bed has also been plotted and it may be noted that the theoritical bed level coincides with the surface level of the bed.

c. General observations

The roughness concentration has a major influence on the roughness factors. The roughness factor $\frac{K_s}{d}$ is the sum of the roughness contribution by the roughness elements and smooth portion of the bed. The functional form of roughness contribution by the floor and roughness elements can be written according to Einstien (1950) as follows τ_o(Total Area of bed) = τ_{o_f} (Area of smooth portion of bed) + τ_{o_r} (Area of Roughness element) In which τ_o is combined shear stress of smooth portion of bed and roughness elements on the bed. Suffix 'f' and 'r' represent smooth and rough bed respectively. Dividing the above expression by totalarea of bed, one can re-write it in terms of concentration

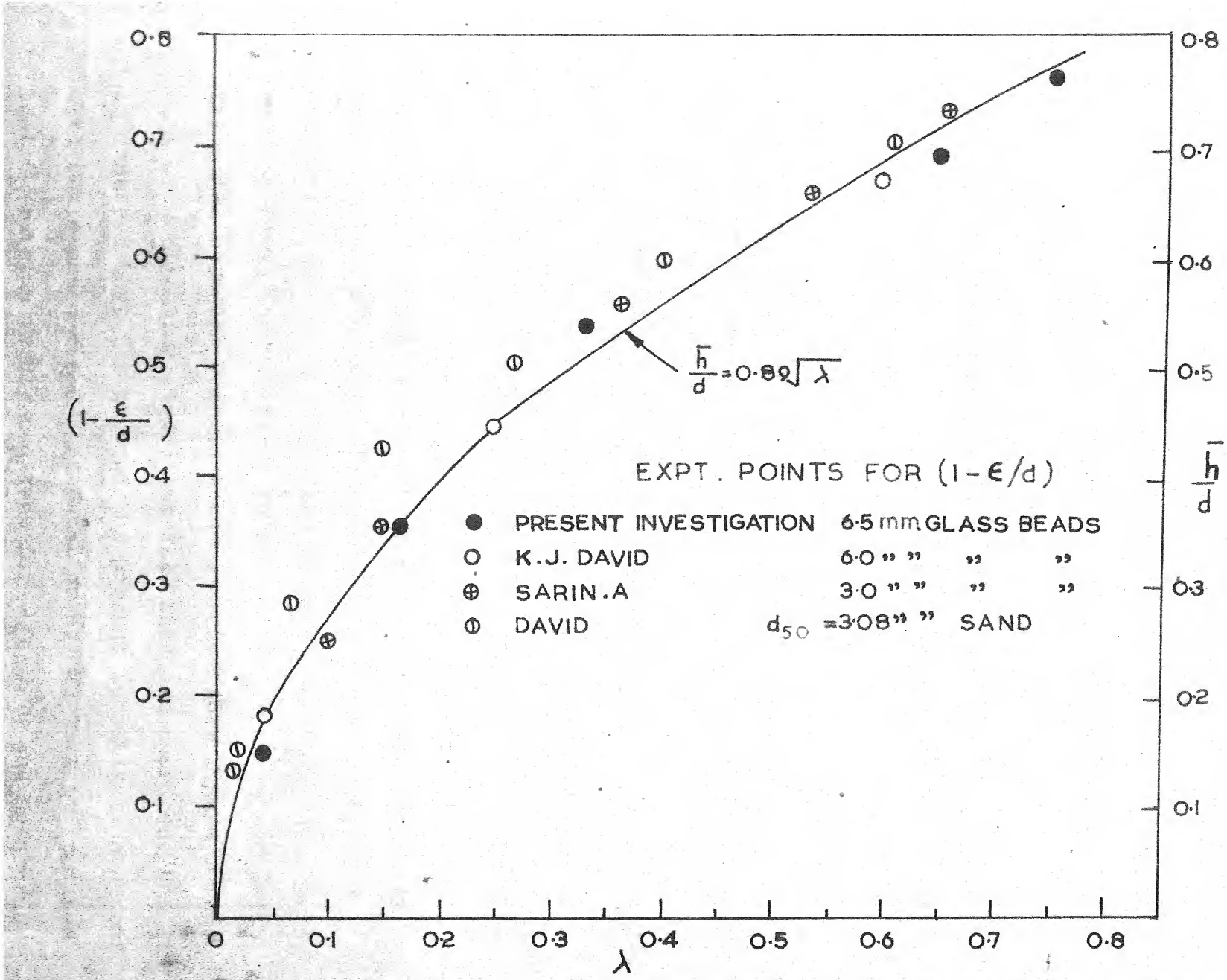

FIG.9 THE EFFECT OF ROUGHNESS CONCENTRATION ON THEORETICAL BED LEVEL

$$\tau_o = \tau_{of}\,\lambda_f + \tau_{or}\,\lambda_r \qquad (1)$$

Since the projected area of roughness element is equal to Plan area of roughness element and it can be related as $\lambda_f = 1 - \lambda_r$ using this relation in equation (2), and denoting $\lambda_r = \lambda$

$$\frac{\tau_{or}}{\tau_o} = \frac{\tau_{of}}{\tau_o}\left(\frac{1-\lambda}{\lambda}\right) - \frac{1}{\lambda} \qquad (3)$$

$\frac{\tau_{of}}{\tau_o}$ remains fairly constant for given flow condition . The ratio $\frac{\tau_{or}}{\tau_o}$ will be a function of λ and this functional form has been plotted in fig. 10. It may be observed that τ_{or} increases with decrease of λ, τ_{or} represents the shear stress offered by single roughness element, may be considered as its drag force. This may be related with the drag coeffecient C_D and velocity of flow u_ε at the top of roughness element, as given below:

$$\tau_{or} = \frac{\text{Drag Force}}{\text{projected area.}} = \frac{1}{2}\rho u_\varepsilon^2 C_D \qquad \ldots(4)$$

The velocity u_ε may be computed by using wall law equation.

$$u_\varepsilon = V_*\left(\frac{1}{\kappa}\,\text{In}\,\frac{\varepsilon}{k_s} + B\right) \qquad \ldots(5)$$

knowing the values of ε, ks and $B_r = 8.5$ for rough turbulent flows, the u_ε, velocity on the top of roughness element is computed. C_D, Drag coeffecient was computed by using this velocity u_ε and has been plotted against λ in Fig. 11. The data of David (1980), Sarin (1980) for glass beads and David for sands has also been in corpora-ted in this figure. The data of Schlichting (1937) has also been incorporated. Now it is observed that the data of the present investigation agre with David and Sarin expirimental data. Further it is noted that C_D remains fairly constant for $\lambda < 0.10$ and decreases

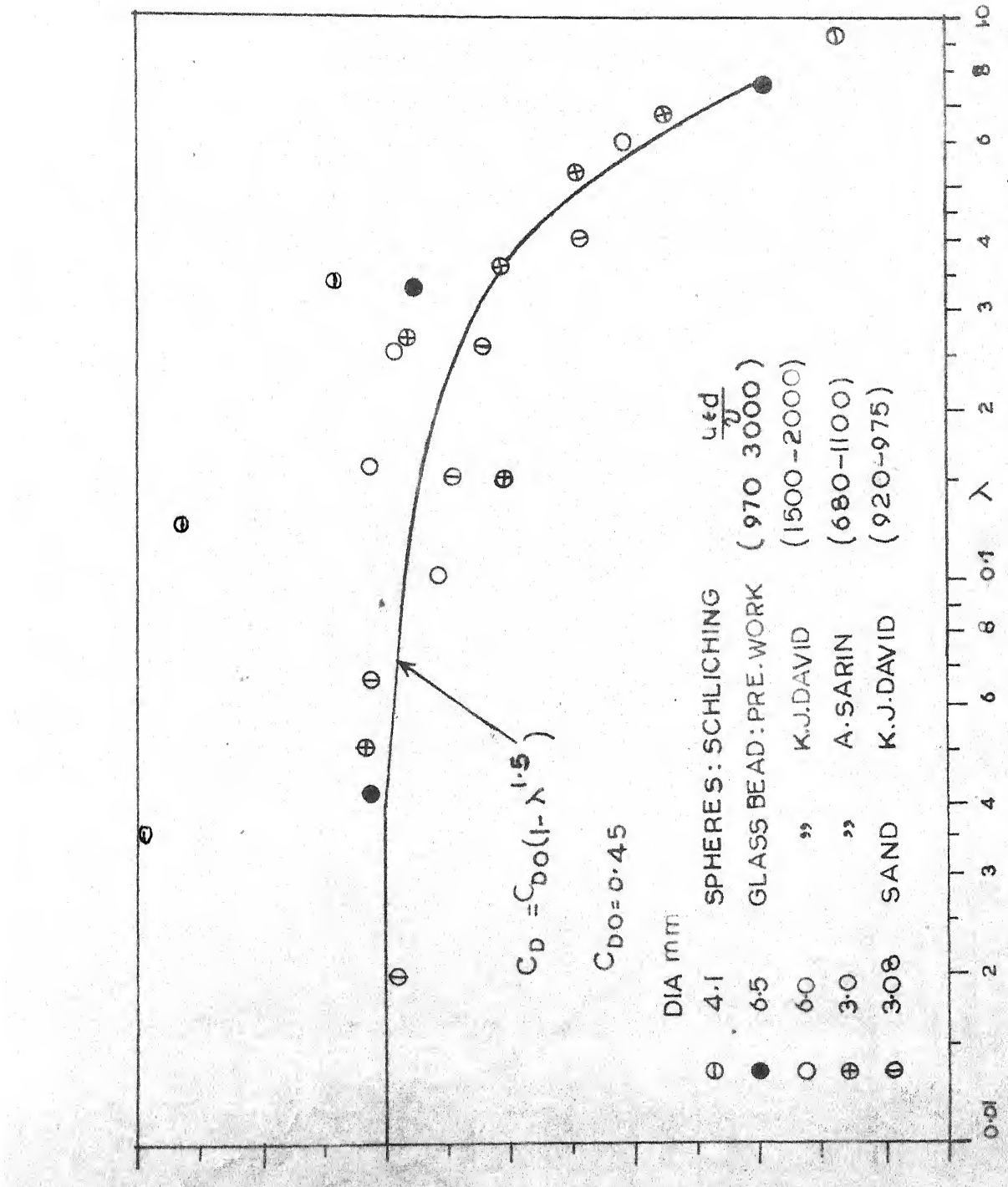

FIG.11 EFFECT OF ROUGHNESS CONCENTRATION ON THE DRAG CO-EFFICIENT OF A SINGLE ROUGHNESS ELEMENT

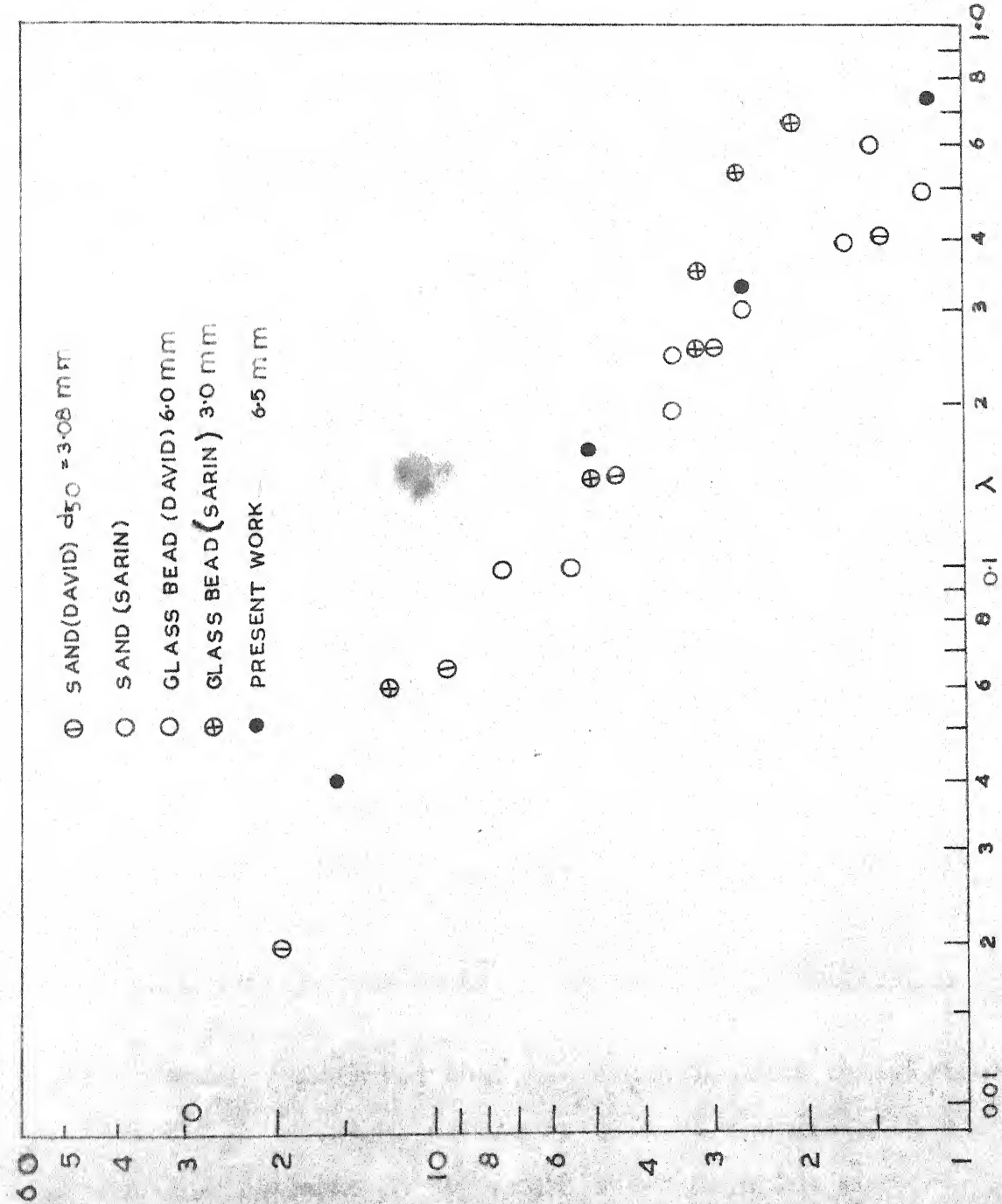

FIG·10 EFFECT OF ROUGHNESS CONCENTRATION ON BED SHEAR STRESS CONTRIBUTED BY ROUGHNESS ELEMENTS

with further increase in λ. An emperical equation for this curve may be written as $C_D = C_{D_0}(1-\lambda^{1.5})$ (where C_{D_0}= 0.45). The value of C_D for $\lambda < 0.1$ fairly coincides with the values calculated. by Neil L. Coleman (1967) in the rough turbulent zone. The computed value of C_D from Schlichting data do not agree with the present investigation. Reason may be attributed to the absence of information on theoritical bed level and hence on the velocity u_ε.

The variation of drag co-effecient C_D with roughness concentration λ infer the variation in the magnitude of fluid dynamic force acting on the roughness element. The fluid dynamic force may be resolved into drag force parallel to flow and lift force perpendicular to flow. Chepil points that the ratio of the magnitude of lift force and drag force for roughness element resting on a bed remains fairly constant. Hence it may be stated that the fluid dynamic force acting on the roughness element decreases as its concentration on the bed increases. This may result in the need of more fluid velocity near the bed, or the shear stress to cause the grain to move as the grain concentration increases.

2. Effecct of Roughness concentration on Initiation of motion:

Shields proposed that the dimensionless shear stress $\tau_* = V_*^2/\left(\frac{\rho_s}{\rho} - 1\right) gd$ necessary to move the grain on stream bed dependes on the grain shear Reynolds number $R_* = \frac{V_* d}{\nu}$. However, it has been found by White (1940) that

factor of relative packings of roughness elements alter the initiation criterion proposed by Shields (1936)

The initiation of motion of 6.5mm diameter glass bead for different density beds λ = 0.0414, 0.166, 0.332 and 0.753 is observed. The experiments were repeated for number of times by varying the slope, discharge and depth of flow to obtain the critical condition. The velocity distribution were carried out for the condition when the roughness element moved out from its position. From this velocity distribution shear volocity V_* and other roughness parameters were computed. Using these computed values the Shields parameter τ_* and R_* are computed and plotted in Fig 12. The data of David (1980) and Sarin for glass bead and sand have also been incorporated. It can be observed from this figure that all data of varying density falls systamiatically in between the data of densest and smooth bed, and it is observed that as the roughness dansity increases the curve for smooth bed moves towords the curve for densest bed. The data of densest bed λ = 0.753 of present investigation falls very close to Shields curve. The shear stress offered by single grain τ_{*r} has been ploted against R_* in Fig 13 and it can be observed that data for all roughness beds falls in the limit of Shields curve.

3. <u>Effect of size variation of single particle (glass bead) in given bed on its initiation of motion.</u>

To study the effect of size variation of single roughness

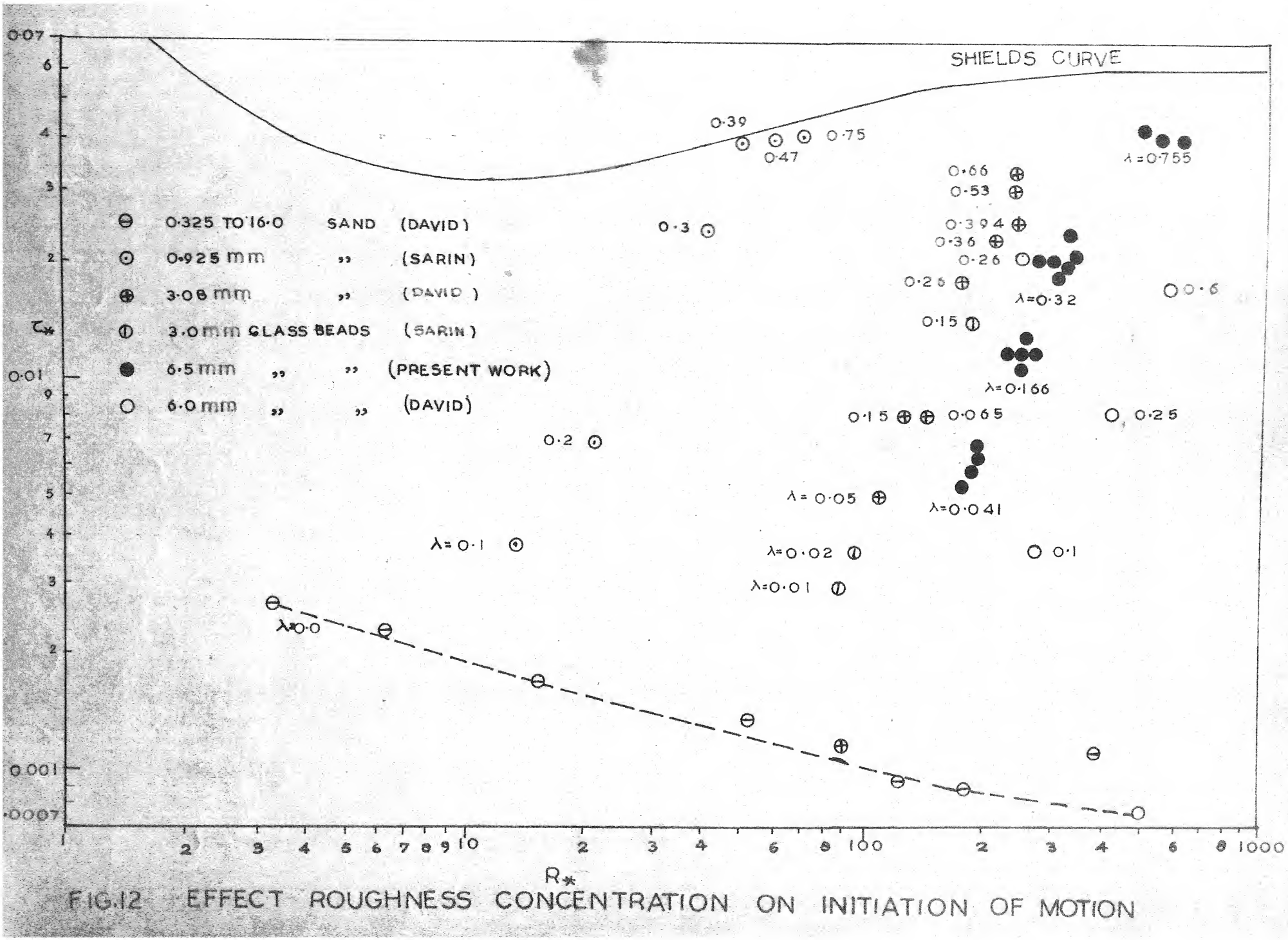

FIG.12 EFFECT ROUGHNESS CONCENTRATION ON INITIATION OF MOTION

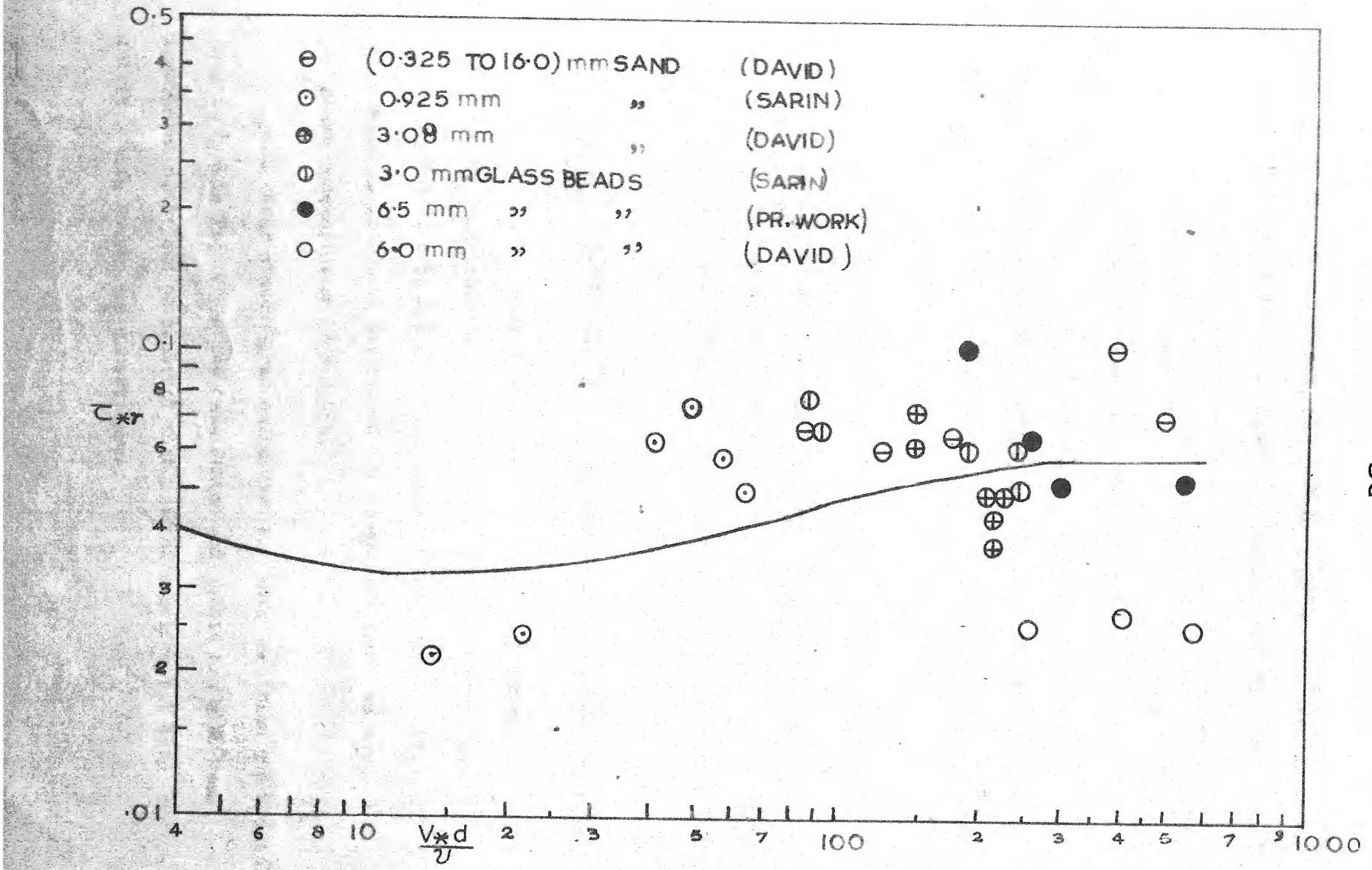

FIG. 13 INITIATION OF MOTION CORRECTED FOR ROUGHNESS CONCENTRATION

element in a given rough bed, on initiation of motion, the size of sediment (d_i) subjected to initiation is changed and for this state of initiation of motion, shear stress τ_{*_i} is calculated and plotted against R_{*_i} in Fig 14 along with Shields curve. The data of David for different rough-beds have also been incorporated. It can be observed that as d_i/d increases τ_{*_i} decreases and the curve shifts towards Shields curve as the roughness density of bed (λ) increases. The shear stress offered by single grain $\tau_{*_{ri}}$ is calculated and plotted against d_i/d in Fig 15. It can be observed that

$$\tau_{*_{ri}} \propto \frac{1}{d_i/d}$$

Calculating the parameter $\tau_{*_{ri}} \sqrt{\frac{d_i}{d}}$ and plotting against d_i/d in Fig 16. It can be observed from this plot that the value of this parameter is almost constant and very close to Shield curve in turbulent zone for present data.

4. Effect of relative protrusion of single particle on its initiation of motion

In order to study this effect, roughness element which is subjected to study the initiation of motion is placed at different levels P_s = d/4, d/3, d/2 above the rough surface, and condition of initiation of motion is determined for these positions on the bed of roughness concentration $\lambda = 0.753$.

The shear states τ_* is calculated for this condition and plotted against P_s/d in Fig 17 and the data Fenton and Abbott has also been incorporated, it can be observed that present experimental data agrees fairly with Fenton and Abbott curve.

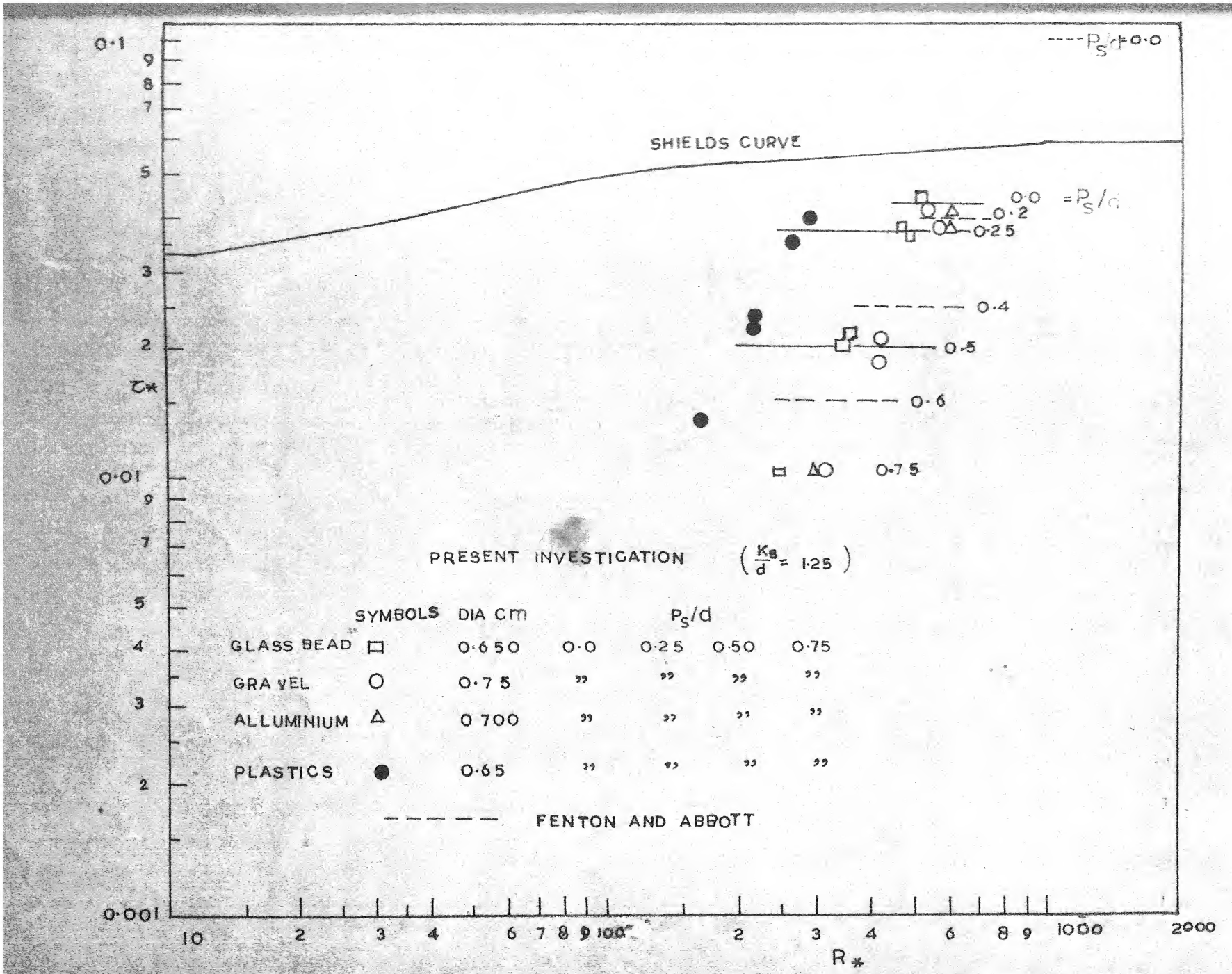

FIG. 18 EFFECT OF RELATIVE POSITION ON INITIATION OF MOTION

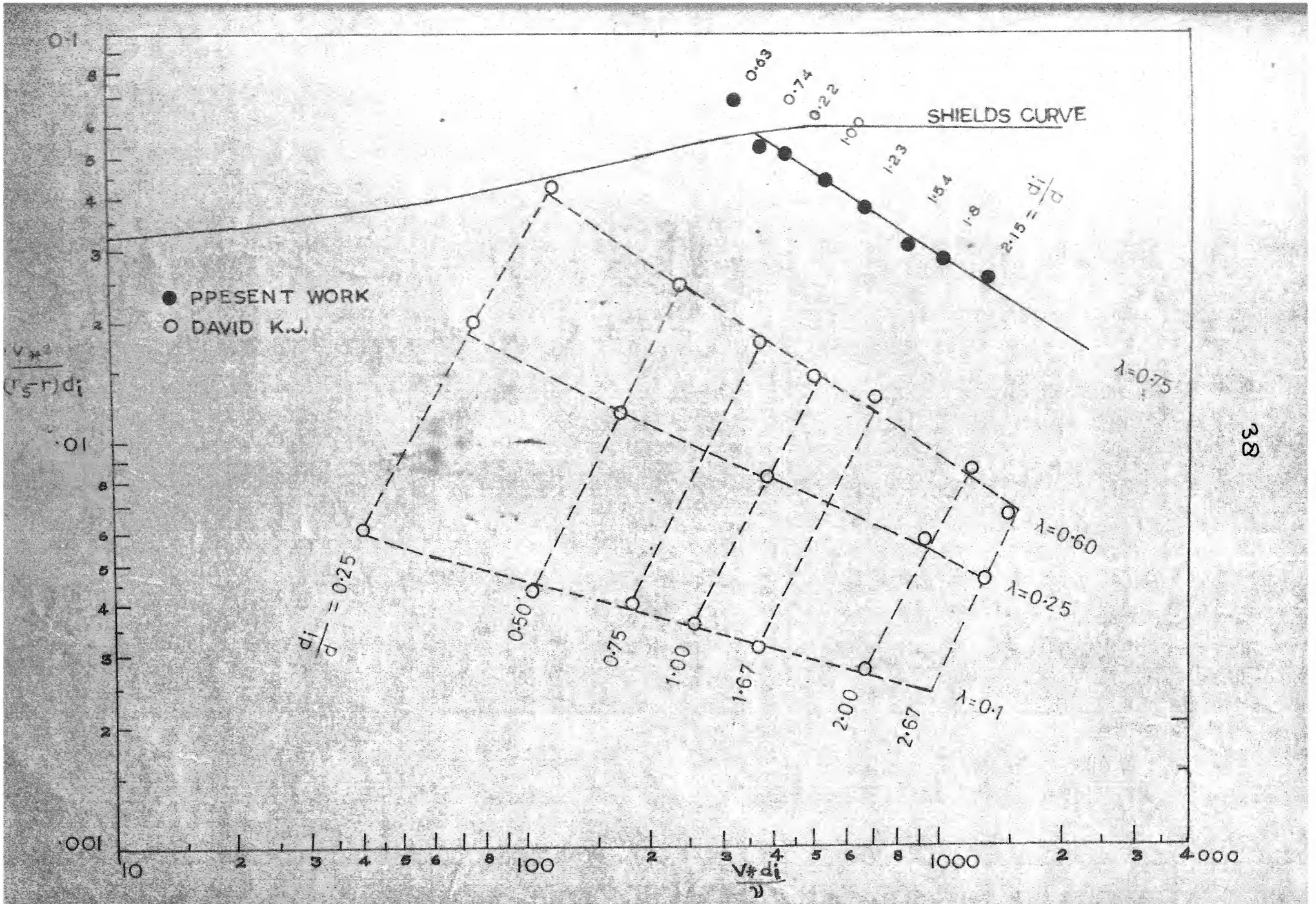

FIG. 14 EFFECT OF SIZE VARIATION ON INITIATION OF MOTION

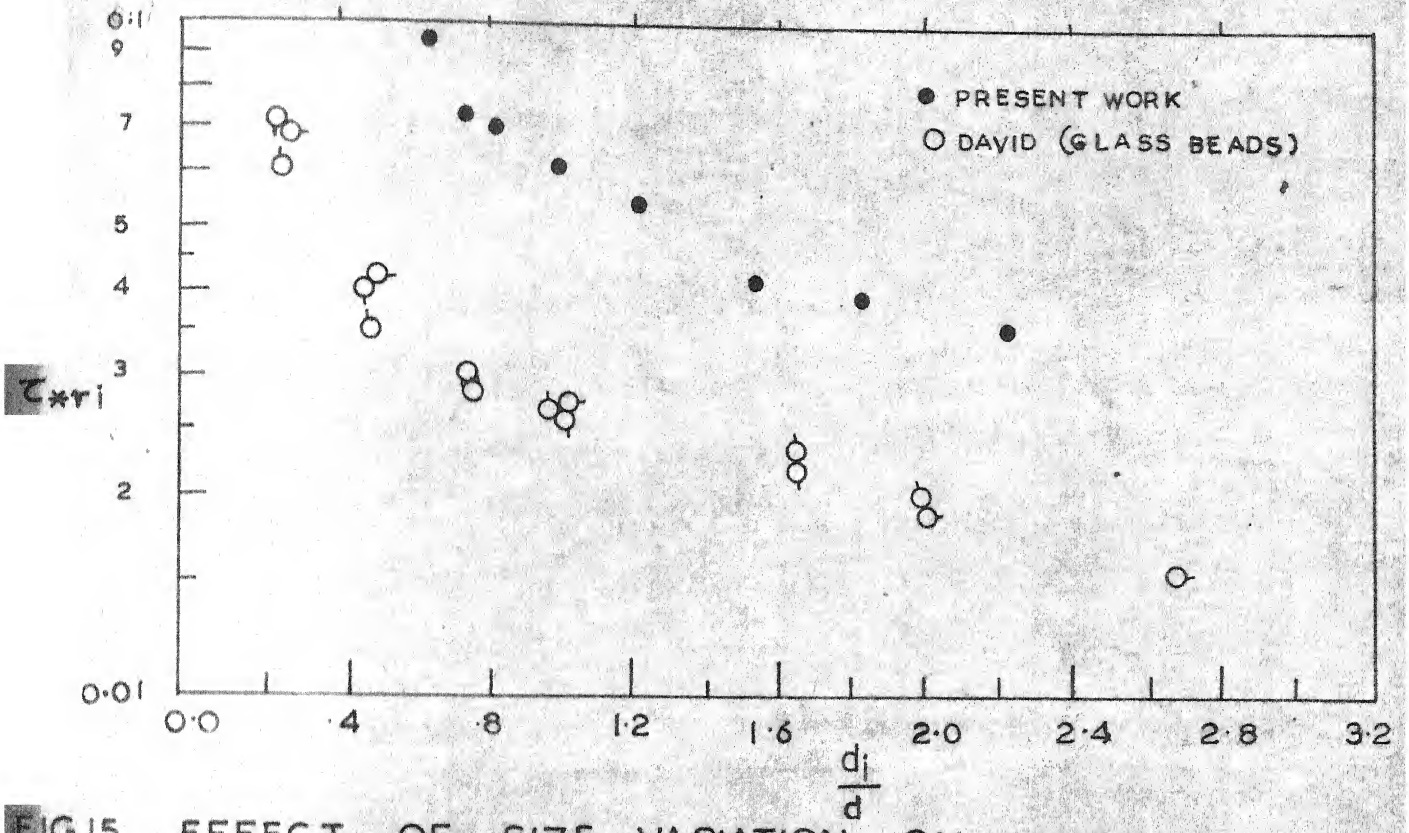

FIG.15 EFFECT OF SIZE VARIATION ON INITIATION OF MOTION IN ROUGH TURBULENT FLOWS

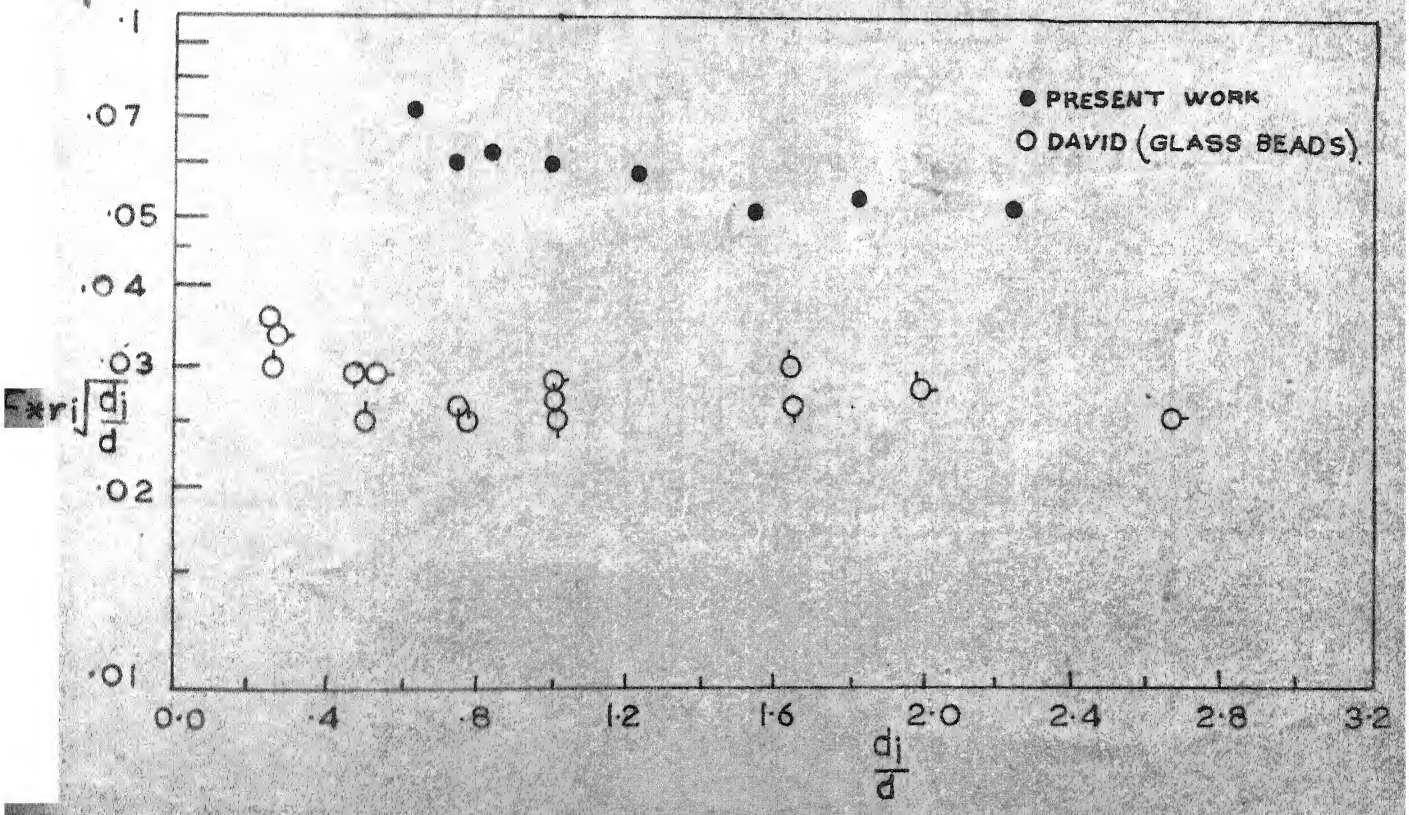

FIG.16 INITIATION OF MOTION AFTER CORRECTION FOR SIZE VARIATION IN ROUGH TURBULENT FLOWS

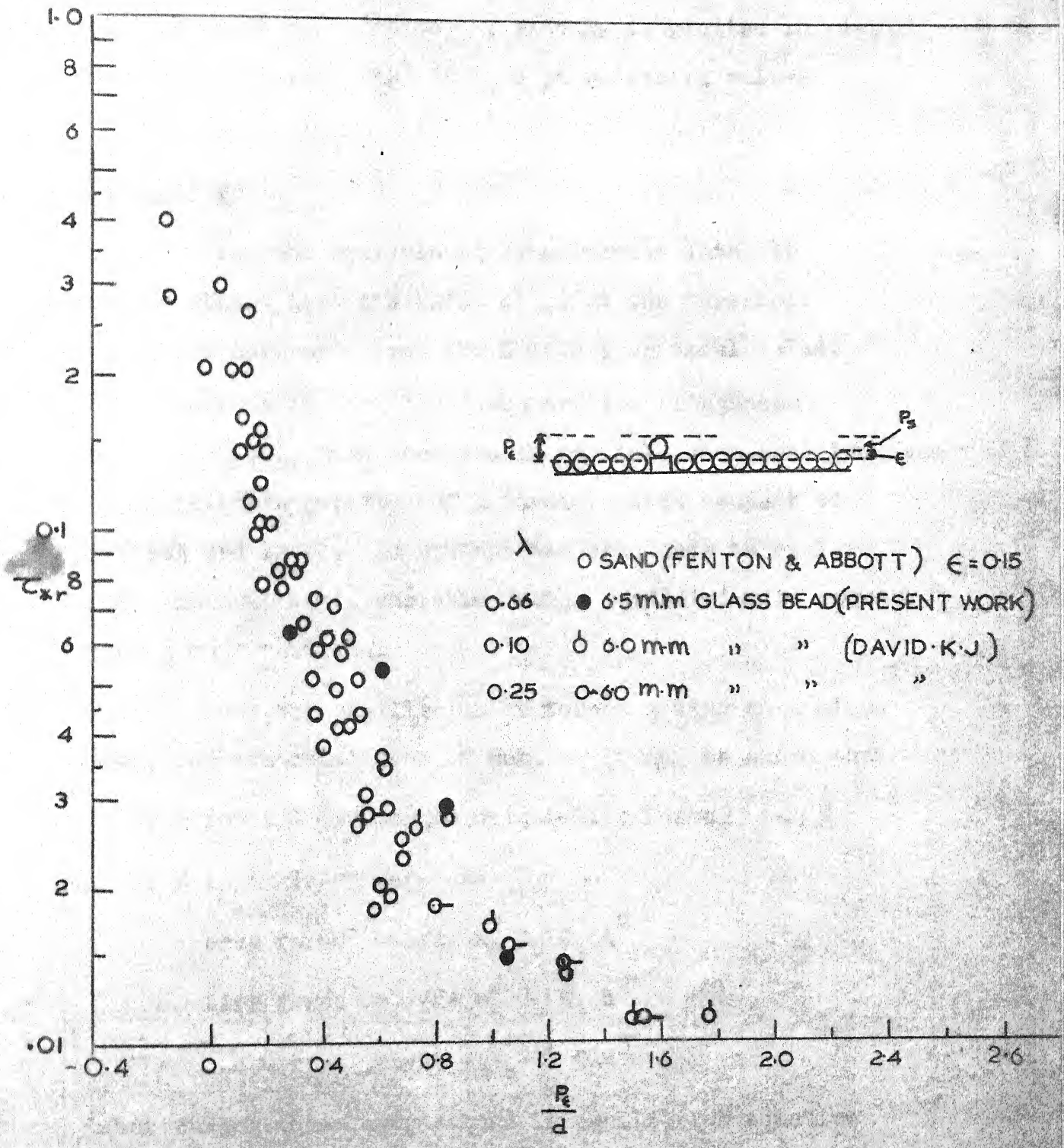

FIG. 17 EFFECT OF RELATIVE POSITION FROM THEORETICAL BEDLEVEL ON INITIATION

For different P_s/d ratios, τ_* with R_* is plotted in Fig.18 it may be observed that as P_s/d increases τ_* values decreases.

Discussions:

From the analysis of experimental data, it may be stated that the value of τ_* at the threshold condition decreases from the Shield's critical value, with decrease in particle concentration (roughness concentration), with increase in particle size, and increase in in relative position of a particle with respect to general bed level. An attempt has been made to explain this characteristic variation using equilibrium of forces acting on a particle.

From the equilibrium of forces acting on a glass bead, for its initiation of motion, it may be shown that

Drag force > (submerged weight-lift force) tan ϕ

where ϕ is angle of response

$$\text{Drag force} = 1/2\rho\, u_e^2\, C_D\, C_1\, d^2$$

$$\text{Lift force} = 1/2\rho\, u_e^2\, C_L\, C_1\, d^2$$

$$\text{ubmerged weight} = (\gamma_s - \gamma)\, C_2 d^3$$

Substituting these expressions in equilibrium equation after rearranging, one gets

$$1/2\rho\, u_e^2\, C_1 d^2\, (C_D - C_L \tan\phi) > (\gamma_s - \gamma)\, C_2 d^3 \tan\phi \quad (6)$$

The velocity u_e at the top of the grain may be computed from equation

$$u_e = V_* \left(\frac{1}{\kappa} \ln \frac{P_e}{k_s} + B \right)$$

Value of constants C_1 and C_2 depends upon the shape of the particle and for spherical glass bead $C_1 = \pi/4$ and $C_2 = \pi/6$. The angle of repose ϕ depends upon size and angularity of the particle. For spharical glass bead of 6.5 mm diameter ϕ is taken as 45^o.

For initiation of motion of glass bead, the threshold condition may be written as

$$\tau_* = \frac{V_*^2}{(\gamma_s - \gamma)d} > \frac{1.333}{(5.75 \log \frac{P_e}{K_s} + B)^2 (C_D - C_L)} \qquad (7)$$

The threshold condition depends on the position of roughness element with respect to theoretical bed level P_e, the roughness characteristics of bed K_s, the roughness constent B, and coefficient of Drag C_D and coefficient of Lift C_L of the particle.

These parameters vary with the roughness concentration, size of the particle and relative position and the state of flow.

As the roughness concentration decreases from the densest case, the value of Drag coefficient C_D and the relative position of theoretical bed level e/d increases

shown in Fig. 11 and Fig. 3 respectively. The value of roughness scale K_s/d depends upon the roughness concentration as shown in Fig. 8. Variation of Lift coefficient is not known. However, making assumption that the variation of Lift coefficient is similar to Drag coefficient, it may be shown from Equation 7 that τ_* decreases with decrease in roughness concentration. This relationship has been observed experimentally in **Fig.12.**

When the size of particle (di) subjected to threshold condition, incomparision to the size of roughness elements(d) increases, the value of P_e/d also increases. This effect causes the decrease in τ_* with increase in d_i/d, This variation has also been observed experimentally as shown in the Fig. 14.

The increase in relative position (elevation) of the particles, causes increase in P_e/d, This results in decrease of τ_* as P_e/d increases in equation 7 which can be observed also from Fig. 17.

The effect of decrease in roughness concentration, increase in size and increase in relative position causes the threshold values to decrease from the threshold value given by Shields for the densest bed. By representing the threshold condition based on the shear stress offered by particle subjected to motion (τ_*) instead of shear stress of the bed τ_*, it can be seen from Fig. 13 that

τ_* values agrees with Shields values fairly well for all roughness concentrations. This kind of analysis could not be shown for the variation of relative size and relative position of particles because the value of C_D was not calculated for the above cases. From this study it can be brought out that the knowledge on the variation of C_D, C_L , ϵ and K_s are needed to predict the threshold condition of a particular particle. In this direction, attempt should be made for determining C_D and C_L of a particle resting on bed for different relative positions and for different relative sizes.

CHAPTER- 4

CONCLUSIONS

A study on the effect of roughness concentration, size variation and relative position of a single particle on the initiation of motion has been made. Roughness concentrations λ = 0.041, 0.166, 0.332, 0.646 and 0.753 are used in this study. The size of particle (d_i) in comparision of roughness element size (d), namely d_i/d was varied. The relative position of particle P_ε measured from the theoretical bed level, namely P_ε/d was varied.

The effect of size and relative position of a particle on the threshold condition are carried out in the densest roughness concentration of the bed. For each threshold condition, the mean velocity was measured at the test position. All the relevent roughness parametors are deduced from these mean velocity distributions. Based on these experimental observations, the following conclusions are drawn:

(a) Co-effecient of drag: The Co-effecient of drag 'C_D' of roughness element increases with decrease in roughness concentration and remains fairly constant for $\lambda \leqq 0.1$.

(b) Theoretical bed level: Theoretical bed level 'ε' shifts from the wall surface on which roughness elements are attached towards the top surface of roughness elements as roughness concentration increases. It was found that the theoretical bed level coincide with average surface level of a rough bed.

(c) Initiation of motion:

(i) Threshold condition represented by Shields parameter τ_* for rough bed condition decreases with decrease in roughness concentration and attains a value of $\tau_* = 0.01$ for the case of single roughness element on smooth bed. By considering the shear stress offered by individual roughness elements, it is shown that the critical shear stress τ_{*r} coinside fairly with Shields curve.

(ii) It is observed that the shear stress of a single roughness element τ_{*r} resting on the bed, decreases with increase in size of roughness element. The effect of size variation taken in the form $\tau_{*r}\sqrt{\frac{d_i}{d}}$ remains fairly constant and this value agrees with Shields critical shear stress value.

(iii) The critical shear stress τ_{*r} decreases with increase in the relative protrusion P_ϵ/d in the rough turbulent zone. Present experimental results agree with the Fenton and Abbott results.

BIBLOGRAPHY

1. Blinco, P.H. and Partheniades, E. , 'Turbulent Characteristics in Free Streamflow Over Smooth and Rough Boundaries', Int. Ass. Hydr. Research, J. Hydr. Research Vol.9, No.1, 1971, pp. 43-69.

2. Chang, Y.L., 'Laboratory Investigation of Flume Traction and Transportation', Trans. A.S.C.E., Vol.104, 1939.

3. Clauser, F.H., 'The Turbulent Boundary Layer', Advances in Applied Mechanics, Vol. IV, Academic Press Inc. New York, 1956, pp. 1-52.

4. David, K.J., 'The Effect of Nonuniformity in Grain Size on the Roughness of Sand Bed', A Thesis submitted in partial fulfilment of the requirements for the degree of Doctor of Philosophy to the Department of Civil Engineering, Indian Institute of Technology, Kanpur, (1980).

5. Egiazaraff, I.V., 'Calculation of Nonuniform Sediment Concentration', J.H.D. Proc. A.S.C.E., Vol.91, No. Hy.4 , July 1965.

6. Einstein, H.A. and Barbarossa, 'River Channel Roughness Trans.' , A.S.C.E., Vol. 117, Paper No. 2528, 1952, pp. 1121-1146, (1952).

7. Fenton and Abbott, 'Initial Movement of Grains on a Stream Bed: The Effect of Relative Protrusion', Department of Civil Engineering, Imperial College London, S.W-7, (1977).

8. Grade, R.J. and Ranga Raju, K.G., 'Mechanics of Sediment Transportation and Alluvial Stream Problems', John Wiley and Sons, Inc., NY. (1977).

9. Hama, F.R., 'Boundary Layer Characteristics for Smooth and Rough Surfaces', Trans. SNANE, Vol.62, (1956).

10. Iwagaki, Y., 'Hydrodynamical Study on Critical Tractive Force', Trans. JSCE, No. 41, 1956 (In Japanese).

11. Kramer, H., 'Sand Mixtures and Sand Movement in Fluvial Models', Trans. ASCE, Vol.100, 1935.

12. Kurihara, M., 'On the Critical Tractive Force', Reports of Research Institute for Hydraulic Engineering, Kyushu University, Vol.4, No.3, Sept. 1948 (in Japanese).

13. Mooye, W.F., 'An Experimental Investigation of the Boundary Layer Development Along a Rough Surface', Ph. Dissertation State University of Iowa.

14. Muller, Albber, Gyr., Themistocles and Dracos, 'A Contribution to Problem of the Threshold of Sediment Transportation', I.A.H.R., Volume, 9-1971, No. 3, p. 373.

15. Neil, L. Colemon, 'A Theoretical and Experimental Study of Drag and Lift Forces Acting on a Sphere Resting on a Hypothetical Streambed', I.A.H.R. 11-14, September 1967, Volume No.3, p. 185 .

16. O'Loughlin, E. Mand Mac Donald, E.G., 'Same Roughness Concentration, Effects on Boundary Resistance', La Houille Blanche, No. 7, 1964,

17. Perry, A.E., Schofield and Jaubert, P.M., 'Rough Wall Turbulent Boundary Layers', Jl. Fluid Mechanics, Vol.37, Part 2, 1969, pp. 383-413.

18. Nikuradse, J., 'Stromungsgestze Rouhen Rohren', Forschugshef 361, V.D.I.

19. Sarin, Alok, 'Roughness of Sand Beds: Effect of Shape and Arrangement Pattern', M.Tech. Dissertation, Indian Institute of Technology, Kanpur.

20. Schlichting, H., 'Experimental Untersuchungen Zum Roughigs Keits Problem', Ingenieur- Archive, Vol. VII, No.1, Fabruary ,1962.

21. Shields, 'Application of Similarity Principles and Turbulence Research to Bed-Load Movement', Translated from: An Wendung dev. Aehnlichkeit smechanik undder Turbulenz forschung auf die Geschiebebewegung', Mitteil-versuch sanstalt fur wasserban nd Schiffbau, Barlin,1936.

22. Vilo, A. Vanoni, 'River Dynamics', Advances in Applied Mechanics; Etd. C.S. Yih, Vol.15, Academic Press,1975, pp. 1-70.

23. White, C.M., 'The Equilibrium of Grains on the Bed of Stream', Proc. R.L.S. Series A, Mathematical and Physical Science No. 958, Vol. 174, Feb. 1940.

24. Aki and Sakai (Ref.8)

25. Sato (Ref.8)

26. U.S.W.E.S. (Ref.8)

APPENDIX

d = 6.5 mm λ = 0.0414 K_s/d = 0.853

e/d = 0.770

Run No.	D cm	δ cm	$\nu \times 10^{+3}$ cm^2/sec	V_* cm/sec.	U_{aug} cm/sec.	$R_* \times 10^{-2}$	$\tau_* \times 10^{+2}$	F_r
1	2	3	4	5	6	7	8	9 10
1.	8.76	3.90	8.80	2.55	31.66	1.88	0.602	0.32
2.	8.76	3.97	8.20	2.26	29.05	1.80	0.548	0.36
3.	10.94	4.43	8.20	2.37	29.36	1.88	0.602	0.28
4.	12.08	3.97	8.20	2.27	28.63	1.88	0.602	0.22
5.	10.40	4.47	8.10	2.23	29.54	1.87	0.584	0.29

λ = 0.166 K_s/d = 3.176

e/d = 0.61

1	2	3	4	5	6	7	8	9 10
6.	11.28	4.92	8.84	3.35	31.17	2.59	1.20	0.30
7.	8.88	5.50	8.84	3.32	-	2.57	1.18	-
8.	12.41	4.42	8.80	3.50	33.70	2.59	1.31	0.31
9.	9.34	5.42	8.80	3.39	33.78	2.50	1.23	0.34
10.	9.35	6.40	8.70	3.83	-	2.89	1.57	-
11.	11.54	5.42	8.70	3.39	31.21	2.72	1.23	0.27

$\lambda = 0.332$ $K_s/d = 3.37$

$\varepsilon/d = 0.46$

1	2	3	4	5	6	7	8	9	10
12	9.92	6.3	2.80	4.62	49.18	3.41	2.29	0.50	
13	11.75	6.3	9.30	4.33	39.91	3.06	2.01	0.37	
14	8.45	7.3	9.20	4.39	41.73	3.10	2.07	0.46	
15	11.75	7.3	9.20	4.28	40.89	3.02	1.96	0.38	
16	10.36	7.3	10.50	4.33	43.80	2.68	2.01	0.43	
17	10.95	7.3	10.50	4.30	44.24	2.68	2.01	0.43	
18	7.47	6.3	10.20	4.33	42.73	2.76	2.01	0.50	
19	9.25	7.3	10.20	4.33	47.15	2.76	2.01	0.50	

A = Aluminium gr= gravel $P_s/d = 0.25$

g = glass P = Plastic $K_s/d = 1.7$

$\lambda = 0.66$ $\varepsilon/d = 0.31$

1	2	3	4	5	6	7	8	9	10
20	6.55	6.55	8.10	5.94	78.93	4.77	3.79	-	0.65 g
21	7.50	7.50	7.90	3.65	66.43	2.94	4.04	0.77	0.625P
22	7.86	6.10	7.80	5.83	63.68	4.68	3.65	0.73	0.650g
23	6.58	6.58	8.00	6.27	78.73	2.90	3.73	0.98	0.750gr
24	5.45	5.10	7.70	6.60	84.84	6.00	3.73	1.16	0.700Al

$\lambda = 0.66$

$P_s/d = 0.50$

1	2	3	4	5	6	7	8	9	10
25	9.47	6.15	8.0	4.11	48.57	3.58	2,09	0.50	0.65 g
26	9.17	6.15	7.9	4.37	49.30	4.17	1.82	0.53	0.75 gr.
27	8.92	8.92	8.0	2.77	43.75	2.20	2.34	0.47	0.625 P
28	11.18	6.90	8.0	4.37	32.80	3.55	2.05	0.31	0.650 g
29	12.90	11.00	7.7	2.73	33.71	2.26	2.27	0.30	0.625 P
30	10.72	7.00	7.8	4.59	38.51	4.43	2.01	0.37	0.750 gr
31	8.25	7.95	7.8	4.92	60.35	4.31	2.07	0.67	0.70 Al

$\lambda = 0.66$

$P_s/d = 0.75$

1	2	3	4	5	6	7	8	9	10
32	10.50	7.00	8.00	3.28	49.61	3.09	1.02	0.48	0.75 g
33	9.35	8.20	8.00	3.43	50.51	3.00	1.01	0.52	0.70 Al
34	9.73	9.10	8.00	3.06	46.62	2.49	1.01	0.48	0.65 g
35	11.50	7.05	8.00	2.11	28.92	1.68	1.36	0.27	0.625 P

$\lambda = 0.753$

$P_s/d = 0.00$

1	2	3	4	5	6	7	8	9	10
36	6.11	5.35	8.00	6.42	63.12	5.22	4.41	0.82	0.65 g
37	6.08	5.85	8.00	6.59	52.81	5.37	4.12	0.68	0.75 gr
38	5.44	4.85	8.00	6.93	63.09	6.06	4.12	0.86	0.70 Al

$\lambda = 0.753$

$P_s/d = 0.65$ cm

1	2	3	4	5	6	7	8	9	10
39	9.48	9.48	8.00	4.48	2,30	3.46	0,405	0,62	
40	9.58	6.90	8.00	5.03	3,02	3,67	0,48	0,74	
41	10.55	7.10	7.90	5.76	3.91	4.36	0,53	0,81	
42	6.11	5.35	8.00	6.42	5,21	4.41	0,65	1,00	
43	4.30	4.30	8.00	6.93	6,92	4,18	0,80	1,23	
44	4.22	4.22	7.95	10.92	13.48	8,31	1,00	1.54	
45	4.15	4.15	7.80	12.06	15.46	10.14	1.10	1.69	

AVERAGE VALUES OF ROUGHNESS FUNCTIONS AND SHEAR STRESS FOR GLASS BEAD BED

Uniform size d = 6.5 mm Arranged in a Systamatic pattern

Sl. No.	λ	e/d	$\frac{\Delta U}{V_*}$	K_s/d	R_x	τ_*	$\frac{\Delta U}{V_*}-5.75\frac{V_* d}{\nu}$
1	0.0414	0.77	9.7	0.853	189.56	6.974×10^{-3}	-3.39
2	0.1660	0.61	13.75	3.176	257.71	1.2462×10^{-2}	-0.114
3	0.3320	0.46	14.48	3.750	292.42	2.150×10^{-2}	+0.300
4	0.6640	0.31	14.10	1.700	486.01	3.648×10^{-2}	-2.500
5	0.7530	0.23	13.30	1.268	539.32	4.220×10^{-2}	-2.400